

## Realistic pseudoscalar-vector Lagrangian. Static and dynamical baryon properties

Ulf-G. Meissner

*Center for Theoretical Physics, Laboratory for Nuclear Science and Department of Physics,  
Massachusetts Institute of Technology, Cambridge, Massachusetts 02139*

N. Kaiser

*Niels Bohr Institute, Blegdamsvej 17, DK-2100 Copenhagen, Denmark*

H. Weigel and J. Schechter

*Department of Physics, Syracuse University, Syracuse, New York, 13244-1130*

(Received 21 November 1988)

We investigate electromagnetic and axial-vector currents and the corresponding form factors as well as meson-nucleon form factors within the framework of a nonlinear chiral Lagrangian constructed by Jain, Johnson, Meissner, Park, and Schechter in Phys. Rev. D 37, 3252 (1988). We employ an unambiguous procedure to construct the electroweak current densities. This brings in a parameter, related to the  $\omega \rightarrow \pi^0 \gamma$  decay rate, which does not appear in the strong-interaction part of the Lagrangian. This results in a fairly accurate description of the nucleons' properties. The effects of coupling to a two-flavor " $\eta$  meson" are shown to be small.

### I. INTRODUCTION

It is now believed that QCD at low energies can be well approximated by an effective chiral Lagrangian made from multiplets of the low-lying meson fields. Baryons are solitonic excitations (Skyrmions) of this Lagrangian. Experiment and the quark model combine to tell us that these low-lying mesons are the pseudoscalar and vector multiplets.

In a previous publication (which we will refer to as I in what follows),<sup>1</sup> we addressed the question of how to construct such a pseudoscalar-vector chiral Lagrangian and determine its parameters. We argued that at present it seems most reasonable to fix the values of the parameters from experiment. Special care has to be taken about the "anomalous" terms proportional to the Levi-Civita tensor  $\epsilon_{\mu\nu\alpha\beta}$ . These terms embody all unnatural-parity meson interactions such as, e.g.,  $\omega \rightarrow \rho\pi$ ,  $\bar{K}K \rightarrow 3\pi$ , . . . . For the appropriate literature on these terms we refer the reader to the reviews.<sup>2,3</sup> The model we discuss here starts out from a general chiral-symmetric Lagrangian of pseudoscalars and vectors first written down in Ref. 4. There appear three unknown strong-interaction constants, two of which we could determine from the strong-interaction processes  $\omega \rightarrow 3\pi$ ,  $\phi \rightarrow \rho\pi$ , and  $\phi \rightarrow 3\pi$ . The third parameter could be estimated from the calculation of some soliton properties. Whereas in I we approximately calculated a few nucleon properties, in this paper we will investigate many more properties and include a discussion of collective quantization.<sup>5</sup> Then a careful investigation of the electromagnetic and weak currents will be performed. In I we noted that when one couples electromagnetism to the strong-interaction Lagrangian, a new term which does not contribute to the strong interactions arises after

suitable "gauging." Its strength parameter ( $d_1$ ) was left unspecified in I. Here, we fix it from the well-known  $\omega \rightarrow \gamma\pi^0$  decay rate. A notable feature in this paper is that all electromagnetic and weak currents are calculated in a uniform way from "first principles." This leads to some new contributions (proportional to  $d_1$ ) which were not previously discussed in the literature.

Since our model is chiral invariant, it obeys exact partial conservation of axial-vector current (PCAC), quite in contrast to the "complete" model<sup>6</sup> and other effective Lagrangians making use of the Bardeen subtracted Wess-Zumino action.<sup>7,8</sup> Further insight into the nucleon structure comes from the calculation of the strong meson-nucleon vertices, which are related to the *ad hoc* strong form factors in one-boson-exchange models of the nucleon-nucleon interaction.

Another issue addressed in I was the influence of an isosinglet-pseudoscalar particle, the  $\eta$  on the properties of the nucleon. We argued that this  $\eta$  will contribute to the moment of inertia of the spinning soliton. However, from the minor influence of the  $\eta$  on the  $NN$  force we conjectured that these effects ought to be small. We will justify this assumption here in presenting a full-scale calculation including the  $\eta$ . Its most prominent effect is to lower the nucleon mass, but by far too little to resolve the main problem of our approach: namely, that with the pion decay constant fixed at its empirical value, the nucleon mass comes out several hundreds of MeV too high.

Our paper is organized as follows. Section II contains a brief review of the strong-interaction Lagrangian. In Sec. III we first briefly review the calculation of the classical soliton performed in great detail in I. Then, the soliton is quantized to give states of good spin and isospin (throughout, we will restrict ourselves to the two-flavor

sector). A careful study of the electromagnetic, axial-vector, and strong properties of the nucleon follows, with detailed numerical results. The outlook is surveyed in Sec. IV. Appendices A and B are technical, while in Appendix C we briefly discuss the induced pseudoscalar form factor. In Appendix D we calculate the parity-violating weak pion-nucleon vertex following the approach outlined in Ref. 9.

## II. LAGRANGIAN OF PSEUDOSCALARS AND VECTORS

Here, we will present the strong-interaction pseudoscalar-vector Lagrangian constructed in Ref. 1. It encodes the two pertinent features of strong-interaction physics at low energy: namely, the spontaneous breakdown of chiral symmetry and the experimental fact that the pseudoscalars and vectors are the lowest-lying multiplets.

In our model the pseudoscalar  $0^-$  nonet  $\phi$  transforms nonlinearly under chiral  $U(3) \times U(3)$ . It is most convenient to use the linearly transforming matrix

$$U = \exp \left[ \frac{i\phi}{f_\pi} \right] \quad (2.1)$$

with  $f_\pi = 93$  MeV the weak pion decay constant. Note that in the present paper we are making some minor changes in notation compared to I. These will be summarized at the end of this section. We will also use

$$\xi = \sqrt{U} = \exp \left[ \frac{i\phi}{2f_\pi} \right]. \quad (2.2)$$

The vector-meson nonet matrix  $\rho_\mu$  is related to the auxiliary "gauge fields"  $A_\mu^L$  and  $A_\mu^R$  by

$$A_\mu^L = \xi \rho_\mu \xi^\dagger + \frac{i}{g} \xi \partial_\mu \xi^\dagger, \quad (2.3a)$$

$$A_\mu^R = \xi^\dagger \rho_\mu \xi + \frac{i}{g} \xi^\dagger \partial_\mu \xi, \quad (2.3b)$$

with  $g$  a coupling constant to be determined later. Obviously,  $A_\mu^L$  and  $A_\mu^R$  are related by the constraint  $A_\mu^L = U A_\mu^R U^\dagger + (i/g) U \partial_\mu U^\dagger$ .

The action built from the pseudoscalars and vectors contains three pieces:

$$\Gamma = \int (\mathcal{L}_1 + \mathcal{L}_2) d^4x + \Gamma_3 = \Gamma_{na} + \Gamma_3. \quad (2.4)$$

The nonanomalous piece  $\Gamma_{na}$  consists of (for a more thorough discussion the reader should consult I)

$$\mathcal{L}_1 = -\frac{1}{2} \text{Tr} [F_{\mu\nu}(\rho) F^{\mu\nu}(\rho)], \quad (2.5)$$

$$\begin{aligned} \mathcal{L}_2 = & m_\rho^2 \text{Tr}(\rho_\mu \rho^\mu) + 2ig_{\rho\pi\pi} f_\pi^2 \text{Tr}[\rho^\mu (\partial_\mu \xi \xi^\dagger + \partial_\mu \xi^\dagger \xi)] \\ & + \frac{1}{2} f_\pi^2 (k+1) \text{Tr}(\partial_\mu \xi \partial^\mu \xi^\dagger) \\ & - \frac{1}{2} f_\pi^2 (k-1) \text{Tr}(\xi^\dagger \partial_\mu \xi \xi \partial^\mu \xi^\dagger) \end{aligned}$$

with  $F_{\mu\nu}(\rho) = \partial_\mu \rho_\nu - \partial_\nu \rho_\mu - ig[\rho_\mu, \rho_\nu]$  where we have identified the gauge-coupling  $g$  with the  $\rho\pi\pi$  coupling

constant,  $g_{\rho\pi\pi} = g \approx 6$  (Ref. 10). The constant  $k$  is given by

$$k = \frac{4g_{\rho\pi\pi}^2 f_\pi^2}{m_\rho^2} \quad (2.6)$$

and follows to be  $k \approx 2.20$  for the empirical values of  $m_\rho$ ,  $f_\pi$ , and  $g_{\rho\pi\pi}$ . For simplicity, we will use, however, the value  $k=2$ , so that we recover the KSRF formula.<sup>11</sup> Notice that the KSRF relation is reasonably well satisfied by experiment, but not required in the present model. The nonanomalous action (2.5) was first written down by Kaymakcalan and Schechter<sup>4</sup> and is equivalent to the hidden-symmetry approach of Bando, Kugo, and Yamawaki.<sup>12</sup> This equivalence has been demonstrated by various authors.<sup>6,13</sup>

The third piece in (2.4), the anomalous action  $\Gamma_3$ , contains terms proportional to the antisymmetric Levi-Civita tensor  $\epsilon_{\mu\nu\alpha\beta}$ . It is most convenient to use the notation of differential forms. Introducing the left-handed nonet one-form

$$\alpha = (\partial_\mu U) U^{-1} dx^\mu = dU U^{-1}, \quad (2.7)$$

the action  $\Gamma_3$  reads

$$\begin{aligned} \Gamma_3 = & \Gamma_{WZ}(U) \\ & + \int \text{Tr} \left[ ic_1 \sqrt{2} (A_L \alpha^3) \right. \\ & + 2c_2 (dA_L \alpha A_L - A_L \alpha dA_L + A_L \alpha A_L \alpha) \\ & \left. + 2\sqrt{2} c_3 \left[ -2i A_L^3 \alpha + \frac{1}{g} A_L \alpha A_L \alpha \right] \right], \end{aligned} \quad (2.8)$$

where  $c_1$ ,  $c_2$ , and  $c_3$  are constants whose values will be specified later on.  $\Gamma_{WZ}(U)$  is the conventional Wess-Zumino term of pseudoscalars.<sup>14</sup> Actually, (2.8) is equivalent to the anomalous action obtained within the "hidden-symmetry approach" by Fujiwara *et al.*<sup>15</sup> when one imposes charge-conjugation invariance as discussed in I and also in Ref. 16. All calculations include a chiral-symmetry-breaking mass term  $\mathcal{L}_{SB} = \frac{1}{4} f_\pi^2 m_\pi^2 \text{Tr}(U + U^\dagger - 2)$ .

In I, we have obtained values for two of the three unknown constants appearing in (2.8) from purely strong-interaction processes: namely, the decays  $\phi \rightarrow \rho\pi$ ,  $\phi \rightarrow 3\pi$ , and  $\omega \rightarrow 3\pi$ . In particular, expanding the action (2.8), one finds vector-vector-pseudoscalar and vector-(pseudoscalar)<sup>3</sup> coupling terms, which have the following coupling strengths:

$$\Gamma_3 = \int [-g_{V\phi} \text{Tr}(d\rho d\rho\phi) + ih \text{Tr}(\rho d\phi d\phi d\phi)] + \dots, \quad (2.9)$$

$$g_{V\phi} = \frac{2\sqrt{2}ic_2}{f_\pi}, \quad h = -\frac{2\sqrt{2}i}{f_\pi^3} \left[ c_1 - \frac{\sqrt{2}c_2}{g} - \frac{c_3}{g^2} \right].$$

For the empirical value of the  $\omega\phi$ -mixing angle,  $|\epsilon| = 0.053 \pm 0.030$ , one finds

$$\begin{aligned} \tilde{g}_{VV\phi} &= \sqrt{2} f_\pi g_{VV\phi} = \pm 1.9, \\ \tilde{h} &= 2\sqrt{2} f_\pi^3 h = \pm 0.4. \end{aligned} \quad (2.10)$$

Within the experimental uncertainties, we can have  $\tilde{g}_{VV\phi} = \pm 1.3, \dots, \pm 2.2$  and  $\tilde{h} = \mp 0.15, \dots, \pm 0.7$ , with the correlation  $|\tilde{g}_{VV\phi} - \tilde{h}| \simeq 1.5$ . It should be noted that one parameter has been left unspecified; however, from our estimate of nucleon properties in I we argued that  $\kappa = 0.12c_3/c_2 \approx 1$ . We will come back to this point when we discuss the static and dynamical properties of the nucleon which will be presented in the following sections.

Here, we will not explore the full U(3) content of the action (2.4), but rather restrict ourselves to the study of nonstrange baryons. Therefore, we will only consider the chiral U(2) × U(2) symmetry of the anomalous action. The pseudoscalar- and vector-meson nonets read

$$\rho = \frac{1}{2}\omega \mathbf{1} + \frac{1}{2}\boldsymbol{\tau} \cdot \boldsymbol{\rho}, \quad \phi = \text{“}\eta\text{”} \mathbf{1} + \boldsymbol{\tau} \cdot \boldsymbol{\pi}, \quad (2.11)$$

where “ $\eta$ ” is an isosinglet pseudoscalar which does not have any  $\bar{s}s$  component. We do not expect the  $\eta$  to play an important role as the  $\pi$ ,  $\rho$ , and  $\omega$  as discussed in some detail in I. Introducing the one-forms

$$\begin{aligned} p &= \xi^\dagger d\xi + d\xi \xi^\dagger = \hat{p} + \frac{i}{f_\pi} d\eta, \\ v &= \xi^\dagger d\xi - d\xi \xi^\dagger, \end{aligned} \quad (2.12)$$

the U(2) reduction of  $\Gamma_3$  can be most easily accomplished. In the two-flavor limit, the result is given in (5.6) of I. Here we note that a term  $(2ic_2/f_\pi)d\eta\omega d\omega$  was omitted there.

Finally, we summarize the changes in notation between this paper and I:

$$\begin{aligned} F_\pi^I &= \sqrt{2} f_\pi^{\text{II}}, \quad g^I = \frac{g^{\text{II}}}{\sqrt{2}}, \quad \phi^I = \frac{\phi^{\text{II}}}{\sqrt{2}}, \\ (\rho^I, A_{L,R}^I) &= \sqrt{2} (\rho^{\text{II}}, A_{L,R}^{\text{II}}), \\ (p_\mu q_\mu)^I &= -(p_\mu q_\mu)^{\text{II}}, \\ G(r)^I &= -G(r)^{\text{II}}, \\ \omega(r)^I &= -\omega(r)^{\text{II}}. \end{aligned} \quad (2.13)$$

The symbols in this paper are denoted by II.

### III. BARYON PROPERTIES IN A SOLITON MODEL APPROACH

#### A. Classical solutions and semiclassical quantization

Following the Skyrme-Witten point of view, baryons emerge as solitons in a purely mesonic theory. As a first step in this approach the static soliton configuration which minimizes the energy must be found. For the model Lagrangian discussed in Sec. II this procedure has been explained in detail in I. Here we want to briefly summarize this calculation without citing the lengthy formulas. Inserting the following hedgehog *Ansätze*

$$U(\mathbf{r}) = \exp[i\boldsymbol{\tau} \cdot \hat{\mathbf{r}} F(r)], \quad (3.1a)$$

$$\xi(\mathbf{r}) = \exp[i\boldsymbol{\tau} \cdot \hat{\mathbf{r}} F(r)/2], \quad (3.1b)$$

$$\rho^{i,a}(\mathbf{r}) = \epsilon^{ika} \hat{\mathbf{r}}^k \frac{G(r)}{gr}, \quad (3.1c)$$

$$\omega^\mu(\mathbf{r}) = \omega(r) \delta^{\mu 0} \quad (3.1d)$$

into the Lagrangian yields the hedgehog mass  $M_H$  as a functional of  $F$ ,  $G$ , and  $\omega$ . The corresponding equations of motion obtained by minimizing  $M_H$  are solved together with proper boundary conditions to ensure baryon number  $B=1$  and finiteness of the soliton energy. In I the hedgehog mass  $M_H$ , the topological baryon charge radius  $r_H$ , and the axial-vector constant  $g_A$  as approximately estimated from the pion tail were presented. We use the standard input parameters  $f_\pi = 93$  MeV,  $m_\pi = 138$  MeV,  $m_\rho = m_\omega = m = 770$  MeV and for simplicity we assume the KSRF relation which gives  $g = 5.8545$ . For the central values of parameters  $(\tilde{h}, \tilde{g}_{VV\phi}) = \pm(0.4, 1.9)$  and  $(1/\sqrt{2}g)c_3/c_2 = \kappa = 0$  (1), we find  $M_H = 1.410$  (1.463) GeV,  $r_H = 0.42$  (0.48) fm, and  $g_A = 0.78$  (0.93). For a more detailed discussion of these quantities we refer the reader to Secs. VII and VIII of I.

As a second step the projection onto states of good spin and isospin is carried out. Following the spirit of Adkins, Nappi, and Witten<sup>5</sup> and as outlined in Ref. 6 we perform the time-dependent SU(2) rotation:

$$U(\mathbf{r}, t) = A(t) U(\mathbf{r}) A^\dagger(t), \quad (3.2a)$$

$$\xi(\mathbf{r}, t) = A(t) \xi(\mathbf{r}) A^\dagger(t), \quad (3.2b)$$

$$\boldsymbol{\tau} \cdot \boldsymbol{\rho}^0(\mathbf{r}, t) = \frac{2}{g} A(t) \boldsymbol{\tau} \cdot [\mathbf{K} \xi_1(r) + \hat{\mathbf{r}} \mathbf{K} \cdot \hat{\mathbf{r}} \xi_2(r)] A^\dagger(t), \quad (3.2c)$$

$$\boldsymbol{\tau} \cdot \boldsymbol{\rho}^i(\mathbf{r}, t) = A(t) \boldsymbol{\tau} \cdot \boldsymbol{\rho}^i(\mathbf{r}) i A^\dagger(t), \quad (3.2d)$$

$$\omega(\mathbf{r}, t) = \frac{\phi(r)}{r} \mathbf{K} \times \hat{\mathbf{r}}, \quad (3.2e)$$

where  $U(\mathbf{r})$  and  $\rho^i(\mathbf{r})$  are defined in (3.1) and  $2\mathbf{K}$  is the angular frequency of the spinning soliton  $i\boldsymbol{\tau} \cdot \mathbf{K} = A^\dagger \dot{A}$ . The U(2) reduction of the anomalous action gives rise to the coupling of an isosinglet pseudoscalar  $\eta$  meson. From parity and isospin the *Ansatz* for  $\eta$  is uniquely determined to be

$$\eta(\mathbf{r}) = \mathbf{K} \cdot \hat{\mathbf{r}} \eta(r). \quad (3.3)$$

This and (3.2) lead to the time-dependent Lagrange function

$$L(t) = \int d^3r \mathcal{L} = -M_H + \theta \text{Tr}(\dot{A} \dot{A}^\dagger), \quad (3.4)$$

where  $\theta$  is the moment of inertia:

$$\theta = 4\pi \int_0^\infty \Lambda[F, G, \omega; \xi_1, \xi_2, \phi, \eta] dr, \quad (3.5)$$

with

$$\begin{aligned}
\Lambda[F, G, \omega; \xi_1, \xi_2, \phi, \eta] &= \frac{2}{3} r^2 f_\pi^2 \left[ \sin^2 F + 8 \sin^4 \left[ \frac{F}{2} \right] - 8 \sin^2 \left[ \frac{F}{2} \right] \xi_1 + 3 \xi_1^2 + 2 \xi_1 \xi_2 + \xi_2^2 \right] - \frac{1}{6} \left[ \phi'^2 + \frac{2}{r^2} \phi^2 + m^2 \phi^2 \right] \\
&+ \frac{1}{3g^2} [3r^2 \xi_1'^2 + 2r^2 \xi_1' \xi_2' + r^2 \xi_2'^2 + 4G^2 (\xi_1^2 + \xi_1 \xi_2 - 2\xi_1 - \xi_2 + 1) + 2(G^2 + 2G + 2) \xi_2^2] + \left[ \frac{2\gamma_1}{3} \right] \phi F' \sin^2 F \\
&+ \left[ \frac{\gamma_2}{3} \right] (\phi' \sin F (G - \xi_1 + 2 - 2 \cos F) + \phi \{ F' [2 + (\xi_1 - G - 2) \cos F + 2 \sin^2 F - 2\xi_1 - 2\xi_2] + \sin F (\xi_1' - G') \}) \\
&+ \left[ \frac{2\gamma_3}{3} \right] \phi F' [(G - \xi_1)(1 - \cos F) + (1 - \cos F)^2 - G \xi_1] + \Lambda_\eta, \tag{3.5a}
\end{aligned}$$

$$\begin{aligned}
\Lambda_\eta &= -\frac{1}{12} (r^2 \eta'^2 + 2\eta^2 + r^2 \tilde{m}_\eta^2 \eta^2) - \left[ \frac{\gamma_3}{gf_\pi} \right] \eta' (G + 1 - \cos F)^2 (\xi_1 + \xi_2) - \left[ \frac{\gamma_1}{9gf_\pi} \right] [\eta' (\xi_1 + \xi_2) \sin^2 F + 2\eta F' (G + \xi_1) \sin F] \\
&- \left[ \frac{\gamma_2}{3gf_\pi} \right] (\eta' \{ (G + \xi_1)(G + 1 - \cos F) + (\xi_1 + \xi_2)[(1 - \cos F)^2 - 2G \cos F] \}) \\
&\quad + \eta [\xi_1' (G + 1 - \cos F) + G' (1 - \cos F - \xi_1) + F' \sin F (G + \xi_1)] \\
&+ \left[ \frac{\gamma_2 g}{6f_\pi} \right] [\eta (\phi \omega' - \omega \phi') - \eta' \phi \omega] - \frac{1}{12} m_\pi^2 r^2 (\cos F) \eta^2, \tag{3.5b}
\end{aligned}$$

where the use of  $\gamma_1 = -3\tilde{h}/2\sqrt{2}$ ,  $\gamma_2 = \tilde{g}_{VV\phi}/g$ , and  $\gamma_3 = \kappa\gamma_2$  turns out to be most convenient. A canonical  $\eta$ -mass term proportional to  $\tilde{m}_\eta^2$  has been added to achieve the physical  $\eta$  mass  $m_\eta^2 = \tilde{m}_\eta^2 + m_\pi^2$ . Extremizing the moment of inertia  $\theta$  gives the coupled equations of motion for the excitations  $\xi_1$ ,  $\xi_2$ ,  $\phi$ , and  $\eta$ . Those are given in Appendix A as are the pertinent boundary conditions.

The nucleon mass  $M_N$  and the nucleon- $\Delta(1232)$  mass splitting follow to be

$$M_N = M_H + \frac{3}{8\theta}, \quad M_\Delta - M_N = \frac{3}{2\theta}. \tag{3.6}$$

In Table I we summarize the results for the moment of inertia, the nucleon mass, and the  $N\Delta$  mass splitting together with the moment-of-inertia contribution  $\theta_\pi$  which was used in I to estimate the total moment of inertia. We

see that for the central values of  $\tilde{h}$  and  $\tilde{g}_{VV\phi}$  together with  $\kappa = +1.0$  the results are very similar to the complete model. Furthermore, for all allowed values of  $\tilde{h}$  and  $\tilde{g}_{VV\phi}$  and keeping  $\kappa \simeq 1$ , the nucleon mass comes out too high, with the  $N\Delta$  splitting somewhat too large for the central values. To lower the nucleon mass, one could think of using a large and negative  $\kappa$ . This, however, also leads to a further increase in the  $N\Delta$  splitting, as can be read off from Table I. In particular, for the central values of  $\tilde{h}$  and  $\tilde{g}_{VV\phi}$ , a value of  $\kappa = -1.0$  already leads to  $\theta \sim 0.3$  fm, which is considerably too small. All the numbers given in Table I do not take into account the contribution from the  $\eta$  [i.e., we have set  $\eta(r) = 0$  throughout]. The discussion of the  $\eta$  effects is relegated to a later section, here let us just mention that the  $\eta$  tends to decrease the  $N\Delta$  mass splitting by less than 10 MeV (for the central values). This effect goes in the proper direction, but it is certainly

TABLE I. Baryon masses, the moment of inertia  $\theta$  of the spinning soliton, the contribution from the classical pion field  $\theta_\pi$ , as well as the nucleon mass and the  $N\Delta$  mass splitting are given. For comparison, we also show the results of the complete model. The standard input parameters  $g = 5.8545$ ,  $f_\pi = 93$  MeV,  $m_\pi = 138$  MeV, and  $m_\rho = m_\omega = m = 770$  MeV are used. The  $\eta$  profile is set to zero throughout.

$(\tilde{h}, \tilde{g}_{VV\phi}, \kappa)$	$\theta$ (fm)	$\theta_\pi$ (fm)	$M_N$ (GeV)	$M_\Delta - M_N$ (GeV)
(+0.7, +2.2, 0.0)	0.407	0.309	1.395	0.728
(+0.4, +1.9, 0.0)	0.626	0.534	1.528	0.473
(+0.4, +1.9, +1.0)	0.731	0.717	1.564	0.405
(-0.15, +1.3, 0.0)	1.425	1.372	1.864	0.208
(+0.4, +1.9, -1.0)	0.314	0.137	1.522	0.942
(+0.4, +1.9, -20.0)	0.322	0.213	1.305	0.918
(+0.4, +1.9, -200.0)	0.383	0.296	1.331	0.773
Complete model	0.677	0.692	1.575	0.437

too small to resolve the problem of the too high nucleon mass and  $N\Delta$  splitting. To end this section, let us mention that one could entertain more complicated methods of quantization. Lee and Zahed<sup>17</sup> have proposed a constraint Dirac quantization of  $\pi\rho\omega$  solitons to properly treat the rotational zero modes. Their results, however, indicate only a very mild change in the moment of inertia so that we can consider the method used here as justified. The constraint Dirac quantization of the Lagrangian presented should be investigated in the future but goes beyond the scope of the present paper.

### B. Electromagnetic properties of nucleons

The computation of the electromagnetic current is of practical interest in measuring how accurately the present model describes the real world and also of conceptual interest in the sense that its isoscalar part ("baryon number" current) is usually computed in a different way from the other currents. Here we shall adopt an approach in which all currents are computed in the same way.

It is immediately clear that what is being experimentally measured when we talk about nucleon electromagnetic properties is the coefficient  $J_\mu^{\text{EM}}$  of the photon field  $\mathcal{A}^\mu$  in the term of the effective action

$$-e \int d^4x J_\mu^{\text{EM}} \mathcal{A}^\mu. \quad (3.7)$$

Note that  $J_\mu^{\text{EM}}$  is an effective current which may also depend on  $\mathcal{A}_\mu$ . In order to find the term (3.7) we must "gauge" the total action  $\Gamma(U, A)$  of this model with the electromagnetic field  $\mathcal{A}_\mu$  in such a way that  $\Gamma(U, A, \mathcal{A})$  is gauge invariant. A convenient generalization of this procedure (discussed in detail in Sec. III of I) is to add a full chiral multiplet of external gauge fields  $B_\mu^{L,R}$  and require that the gauged object  $\Gamma(U, A, B)$  yield the well-known non-Abelian chiral anomaly. Using the equation of motion of the external fields it is easy to see that the candidate currents

$$J_\mu^{L,R} \propto \left. \frac{\delta \Gamma(U, A, B)}{\delta B_\mu^{L,R}} \right|_{B=0} \quad (3.8)$$

actually correspond to the zero- $B$ -field limit of formally conserved quantities in our model.

For orientation let us discuss the application of (3.8) to the isoscalar current in the ordinary Skyrme model (where the vector-meson fields  $A$  are deleted). Then the gauged Wess-Zumino term gives a contribution which is identical to the "topological" current originally found by Skyrme.<sup>18</sup> There is the amusing feature that this term does not (in the two-flavor case) contribute to the strong-interaction Lagrangian which is used to study the soliton. A similar phenomenon exists in the present model where the vector mesons are present. The appropriate part of  $\Gamma(U, A, B)$  due to the  $\epsilon$  terms is given in (3.11) of I. The last term of this expression,

$$d_1 \int \text{Tr}[F(B_L)(\alpha_1\alpha_2 - \alpha_2\alpha_1) + F(B_R)(\beta_1\beta_2 - \beta_2\beta_1)], \quad (3.9)$$

where  $F(B_L) = dB_L - ihB_L^2$ ,  $\alpha_i$  and  $\beta_j$  are left- and right-handed one-forms defined in I and  $d_1$  is a new constant, obviously makes no contribution to the strong-interaction part of the Lagrangian. However, it does contribute to the electromagnetic current. We can get a handle on its value by calculating the electromagnetic decay widths for  $\omega \rightarrow \pi^0\gamma$  in this model (equivalently  $\rho^0 \rightarrow \pi^0\gamma$  or some other similar mode could be used). We find the decay width to be

$$\Gamma(\omega \rightarrow \pi^0\gamma) = \frac{e^2}{12\pi} |\mathbf{q}_\pi|^3 \left[ \frac{g}{f_\pi} \right]^2 R^2, \quad (3.10)$$

where  $\mathbf{q}_\pi$  is the daughter pion momentum in the  $\omega$  rest frame and the relevant real linear combination of coupling constants is

$$R = 2 \left[ \frac{d_1}{h} - \frac{ic_2}{g^2} \right]. \quad (3.11)$$

Notice that the ratio  $d_1/h$ ,  $h$  being a coupling constant for the external field multiplet, is what actually enters into our discussion. From the observed width we find

$$|R| = 0.038 \pm 0.002. \quad (3.12)$$

Of course, the sign of  $R$  is undetermined by the above argument.

As an example we now briefly discuss the computation of the time component of the two-flavor baryon-number current. We specialize the external fields to the photon field by setting  $hB_{L,R} \rightarrow eQ\mathcal{A}$ , where the charge matrix  $Q$  has the decomposition  $Q = I_3 + B/2 = \frac{1}{2}\tau_3 + \frac{1}{2}(\frac{1}{3})$ . To apply (3.8) we functionally differentiate the gauged action with respect to the "isoscalar photon:"  $Q\mathcal{A} \rightarrow \mathcal{A}/3$ . Then, also substituting in the classical values of the fields (3.1), we find the current density  $J_0^B$ :

$$\begin{aligned} J_0^B = & -\frac{4gf_\pi^2}{3} \omega(r) - \frac{F'\sin^2 F}{2\pi^2 r^2} + \frac{4\sqrt{2}ic_1}{gr^2} F'\sin^2 F \\ & - \frac{4i}{3g^2} \left[ c_2 + \frac{\sqrt{2}c_3}{g} \right] \frac{F'}{r^2} [3\sin^2 F - (1+G - \cos F)^2] \\ & - \frac{4ic_2}{3g^2 r^2} [F'G(G+2) + 2G'\sin F] \\ & + \frac{8}{3r^2} \frac{d_1}{h} \frac{d}{dr} [-\sin F(G+1) + \frac{1}{2}\sin 2F]. \end{aligned} \quad (3.13)$$

The first term in (3.13) represents the entire contribution from the gauged nonanomalous part of the action while the second term (identical to the original Skyrme result) comes from the gauged Wess-Zumino action.<sup>5</sup> The remaining terms are found from (3.11) in I. The above expression can be simplified by using the classical equation of motion for  $\omega(r)$ . This yields

$$\begin{aligned} J_0^B = & \frac{1}{r^2} \frac{d}{dr} \left[ -\frac{F}{4\pi^2} + \frac{\sin 2F}{8\pi^2} - \frac{2r^2}{3g} \omega' \right. \\ & \left. + \frac{4}{3} R \sin F (\cos F - G - 1) \right], \end{aligned} \quad (3.14)$$

where  $R$  is defined in (3.11). It is interesting that, using (3.12), there are no undetermined parameters in (3.14). We easily verify the normalization condition

$$4\pi \int_0^\infty r^2 dr J_0^B = 1, \quad (3.13)$$

using the boundary conditions on  $F$ ,  $G$ , and  $\omega$ . Note that only the first term in (3.14) contributes at the boundaries. An important point evident from (3.14) is that the relative sign of  $\omega$  and  $F$  is measurable. It was remarked in Sec. VII of I that the sign of  $\omega(r)$  was linked to an overall sign of  $c_1, c_2, c_3$ . Changing both simultaneously leaves the energy functional invariant. There was no way for us to determine the overall sign of  $c_1, c_2, c_3$  from the meson sector. Now, however, we find that only one sign choice for  $\omega(r)$  in (3.14), for example, gives acceptable values for the isoscalar electromagnetic properties so that the overall sign for  $c_1, c_2, c_3$  can be fixed. The appropriate sign choices for our central determination of parameters are

$$\tilde{h} = +0.4 \quad \text{and} \quad \tilde{g}_{VV\phi} = +1.9.$$

The other current components needed for discussing electromagnetic properties of the nucleon,  $J_i^{I=0}, J_0^{I=1}, J_i^{I=1}$ , can be computed from (3.8) in a similar way. Some of these currents will involve also the moment of inertia  $\theta$  as well as the excitations  $\xi_1, \xi_2, \phi$ , and  $\eta$ . After using the semiclassical quantization prescription

$$\sigma = -2i\theta \text{Tr}(A^\dagger \dot{A} \tau), \quad (3.15a)$$

$$\tau = 2i\theta \text{Tr}(\dot{A} A^\dagger \tau), \quad (3.15b)$$

$$\sigma_i \tau_a = -\frac{1}{2} \text{Tr}(A \tau_i A^\dagger \tau_a), \quad (3.15c)$$

the general form of the currents is obtained to be

$$J_0^{I=0} = \frac{1}{2} J_0^B = R_1(r), \quad (3.16a)$$

$$J_i^{I=0} = R_2(r) \epsilon_{ijk} \sigma_j \hat{p}_k, \quad (3.16b)$$

$$J_0^{I=1} = R_3(r) \tau, \quad (3.16c)$$

$$J_i^{I=1} = R_4(r) \epsilon_{ijk} \sigma_j \hat{p}_k \tau. \quad (3.16d)$$

For the model considered here,  $R_1(r)$  can be read off from Eq. (3.14) and  $R_i(r)$ ,  $i=2,3,4$ , are presented in Appendix B. The derivation of the electromagnetic form factors has been described at some length in Ref. 6. There it has been shown that it is most convenient to work in the Breit frame, in which the four-momentum  $q^\mu$  of the virtual photon coupled to the nucleon acquires the specific form  $q^\mu = (0, \mathbf{q})$ . Furthermore, the electric and magnetic parts of the currents separate in this special frame:

$$\langle N_f(\frac{1}{2}\mathbf{q}) | J_0(0) | N_i(-\frac{1}{2}\mathbf{q}) \rangle = G_E(\mathbf{q}^2) \chi_f^\dagger \chi_i, \quad (3.17a)$$

$$\langle N_f(\frac{1}{2}\mathbf{q}) | J_i(0) | N_i(-\frac{1}{2}\mathbf{q}) \rangle = \frac{G_M(\mathbf{q}^2)}{2M_N} \chi_f^\dagger i \sigma \times \mathbf{q} \chi_i, \quad (3.17b)$$

where  $\chi_f$  and  $\chi_i$  are two-component Pauli spinors of the final and initial nucleon states, respectively. Thus in the

Breit frame the form factors  $G_E$  and  $G_M$  are obtained by Fourier transformation of the corresponding electromagnetic currents  $J^{\mu, I=0}$  and  $J^{\mu, I=1}$ . From (3.16) and (3.17) we therefore have

$$G_E^{I=0}(\mathbf{q}^2) = 4\pi \int_0^\infty dr r^2 j_0(qr) R_1(r), \quad (3.18a)$$

$$G_M^{I=0}(\mathbf{q}^2) = 8\pi M_N \int_0^\infty dr r^2 \left[ \frac{r}{q} \right] j_1(qr) R_2(r), \quad (3.18b)$$

$$G_E^{I=1}(\mathbf{q}^2) = 4\pi \int_0^\infty dr r^2 j_0(qr) R_3(r), \quad (3.18c)$$

$$G_M^{I=1}(\mathbf{q}^2) = 8\pi M_N \int_0^\infty dr r^2 \left[ \frac{r}{q} \right] j_1(qr) R_4(r), \quad (3.18d)$$

where  $q = |\mathbf{q}|$  and  $j_i(qr)$  are the spherical Bessel functions. The projection onto proton and neutron states proceeds in the well-known way:

$$G_{E,M}^{p,n} = G_{E,M}^{I=0} \pm G_{E,M}^{I=1}. \quad (3.19)$$

The electric form factors turn out to be properly normalized, i.e.,  $G_E^{p,n}(0) = 1, 0$  while the magnetic form factors at zero-momentum transfer supply the magnetic moments:

$$G_M^p(0) = \mu_p, \quad G_M^n(0) = \mu_n. \quad (3.20)$$

Finally the electromagnetic radii of the proton and nucleon are related to the form factors via

$$\langle r^2 \rangle_E^{p,n} = -6 \frac{d}{d\mathbf{q}^2} G_E^{p,n}(\mathbf{q}^2) \Big|_{\mathbf{q}=0}, \quad (3.21a)$$

$$\langle r^2 \rangle_M^{p,n} = -\frac{6}{\mu_{p,n}} \frac{d}{d\mathbf{q}^2} G_M^{p,n}(\mathbf{q}^2) \Big|_{\mathbf{q}=0}. \quad (3.21b)$$

In Table II the charge radii, the magnetic moments, and the proton and neutron radii are given, together with the isoscalar and isovector magnetic moments for  $R = -0.04$ . For the central values of the parameters with  $\kappa = 0$  or  $\kappa = 1$ , these results are of the same quality as the ones of the complete model. The magnetic moments are a bit too large in magnitude; on the other hand, the neutron electric radius is closer to the empirical value. It is interesting to note that only the neutron charge radius and the isovector magnetic moment vary strongly within the allowed range of  $\tilde{g}_{VV\phi}$  and  $\tilde{h}$ , whereas all other quantities are relatively stable. For comparison, we give in Table III the same quantities for  $R = +0.04$ . As one can see, the overall agreement with the data is clearly worse than in the case  $R = -0.04$ . The electromagnetic form factors of the proton and neutron are shown in Figs. 1–4. In the case of the proton electric form factor, for the central choice of parameters we find that it falls off somewhat faster than the phenomenological dipole fit. The neutron charge form factor displayed in Fig. 2 is obviously most sensitive to parameter variations. It comes out a bit too small for the central choice of parameters ( $\kappa = 0$  or  $\kappa = 1$ ); for  $\kappa = -1$ , however, it is close to the recent semiphenomenological fit of Gari and Krümpelmann.<sup>19</sup> The magnetic form factors show approximately a dipole behavior; it is interesting to note that the  $q^2$  dependence of these form factors shown in Figs. 3 and 4 is very insensitive to the choice of parameters, quite in contrast to

TABLE II. Electromagnetic properties of nucleons for  $R = -0.04$ . the electric and magnetic radii of the proton and neutron as well as their magnetic moments are given. For illustration, we also give the isoscalar and isovector magnetic moments,  $\mu_s$  and  $\mu_v$ , respectively. For comparison, the results for the complete model as well as the empirical data are given.

$(\tilde{h}, \tilde{g}_{VV\phi}, \kappa)$	$r_{E,p}$ (fm)	$r_{E,n}^2$ (fm <sup>2</sup> )	$\mu_s$ (n.m.)	$\mu_v$ (n.m.)	$\mu_p$ (n.m.)	$\mu_n$ (n.m.)	$r_{M,p}$ (fm)	$r_{M,n}$ (fm)
(0.4, 1.9, 0)	1.01	-0.16	0.40	2.50	2.90	-2.10	0.93	0.91
(0.4, 1.9, +1)	1.05	-0.19	0.40	2.80	3.19	-2.40	0.96	0.94
(0.4, 1.9, -1)	0.81	-0.13	0.36	1.58	1.95	-1.22	0.82	0.75
(0.7, 2.2, 0)	0.89	-0.20	0.40	1.52	1.92	-1.13	0.88	0.89
(-0.15, 1.3, 0)	1.17	-0.04	0.38	5.71	6.09	-5.33	1.00	0.96
Complete model	0.97	-0.25	0.47	2.31	2.77	-1.84	0.94	0.94
Expt.	0.86±0.01	-0.119±0.004	0.44	2.35	2.79	-1.91	0.86±0.06	0.88±0.07

electric form factors. Again we should stress that for the central choice of parameters with  $R = -0.04$  and  $\kappa = 0$  (or  $\kappa = 1$ ), the electromagnetic properties of nucleons predicted by this model are similar to the ones obtained in the complete model.<sup>6</sup>

### C. Axial properties of nucleons

The evaluation of the axial-vector current proceeds analogously to the calculation of the electromagnetic current, i.e., by gauging the Lagrangian with an external field,  $\mathbf{a}_\mu$  which now, of course, is axial. Therefore we have to replace the external gauge fields by

$$hB_{\mu,L} \rightarrow \mathbf{a}_\mu \cdot \frac{\boldsymbol{\tau}}{2} \quad \text{and} \quad hB_{\mu,R} \rightarrow -\mathbf{a}_\mu \cdot \frac{\boldsymbol{\tau}}{2}$$

in (3.5) and (3.11) of I. In correspondence to (3.8) the

$$A_1(r) = \frac{f_\pi^2}{r} \sin F (2G + 2 - \cos F) + (\gamma_1 + \frac{3}{2}\gamma_2) \frac{\omega F'}{2r} \sin 2F + \left[ \frac{\gamma_2}{2r} \right] [\omega' \sin^2 F - \omega G' \cos F + \omega' \cos F (1 + G - \cos F)] \\ + (\frac{1}{2}\gamma_2 + \gamma_3) \frac{\omega F'}{r} \sin F (1 + G - \cos F) + \left[ \frac{2g}{r} d_1 \right] (\omega' \sin^2 F + \omega F' \sin 2F), \quad (3.24a)$$

$$A_2(r) = -A_1(r) + f_\pi^2 F'(r) + (\gamma_1 + \frac{3}{2}\gamma_2) \omega \frac{\sin^2 F}{r^2} - \left[ \frac{\gamma^2}{2r^2} \right] \omega G (G + 2) + (\frac{1}{2}\gamma_2 + \gamma_3) \frac{\omega}{r^2} (1 + G - \cos F)^2 + 4g \frac{d_1}{h} \omega \frac{\sin^2 F}{r^2}. \quad (3.24b)$$

Note that the KSRF relation has been used to simplify the first term of (3.24a).

Again as in the case of the electromagnetic currents a term proportional to  $d_1$  shows up. Such a term would

axial-vector current  $\mathbf{A}_\mu$  is derived from

$$\mathbf{A}_\mu = \frac{\delta \Gamma(U, A_L, \mathbf{a})}{\delta \mathbf{a}^\mu} \Big|_{\mathbf{a}=0}. \quad (3.22)$$

In order to calculate the axial form factor it is sufficient to consider the spatial components  $\mathbf{A}_i$  because a careful treatment of the semiclassical quantization gives a vanishing matrix element for the time component of the axial-vector current between nucleon states (i.e., no second-class currents as shown in Ref. 6). After substituting in the soliton profiles we have

$$A_{ia} = [A_1(r) \delta_{ib} + A_2(r) \hat{r}_i \hat{r}_b] \frac{1}{2} \text{Tr}[A \tau^b A^\dagger \tau^a], \quad (3.23)$$

wherein the radial functions  $A_1(r)$  and  $A_2(r)$  are obtained as

have been missed if the axial-vector current had been computed from just the strong-interaction part of the Lagrangian.

Next, we calculate the axial form factor  $G_A(\mathbf{q}^2)$  of the

TABLE III. Electromagnetic properties of nucleons for  $R = +0.04$ . Notations as in Table II.

$(\tilde{h}, \tilde{g}_{VV\phi}, \kappa)$	$r_{E,p}$ (fm)	$r_{E,n}^2$ (fm <sup>2</sup> )	$\mu_s$ (n.m.)	$\mu_v$ (n.m.)	$\mu_p$ (n.m.)	$\mu_n$ (n.m.)	$r_{M,p}$ (fm)	$r_{M,n}$ (fm)
(0.4, 1.9, 0)	0.90	-0.33	0.33	3.09	3.43	-2.76	0.80	0.81
(0.4, 1.9, 1)	0.96	-0.34	0.42	3.64	4.06	-3.22	0.81	0.83
(-0.15, 1.3, 0)	1.06	-0.24	0.44	7.53	7.97	-7.09	0.86	0.85
(0.7, 2.2, 0)	0.80	-0.32	0.30	1.78	2.08	-1.48	0.78	0.82

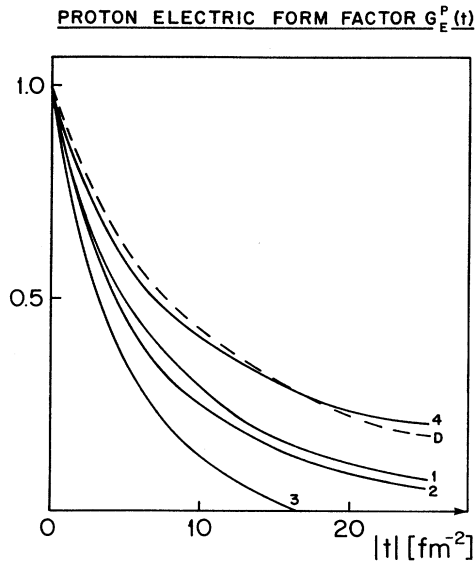


FIG. 1. Proton electric form factor for various parameter sets of  $\{\tilde{h}, \tilde{g}_{VV\phi}, \kappa\}$ . We define  $1 \equiv \{0.4, 1.9, 0\}$ ,  $2 \equiv \{0.4, 1.9, 1\}$ ,  $3 \equiv \{-0.15, 1.3, 0\}$ , and  $4 \equiv \{0.7, 2.2, 0\}$ . In all cases  $R = -0.04$  which fixes  $d_1/h$  according to Eq. (3.11).  $D$  denotes the empirical dipole fit  $G_E^p(t) = (1 + |t|/0.71 \text{ GeV}^2)^{-2}$ . The standard input  $f_\pi = 93 \text{ MeV}$ ,  $m_\rho = m_\omega = m = 770 \text{ MeV}$ , and  $m_\pi = 138 \text{ MeV}$  is used.

NEUTRON ELECTRIC FORM FACTOR  $G_E^n(t)$

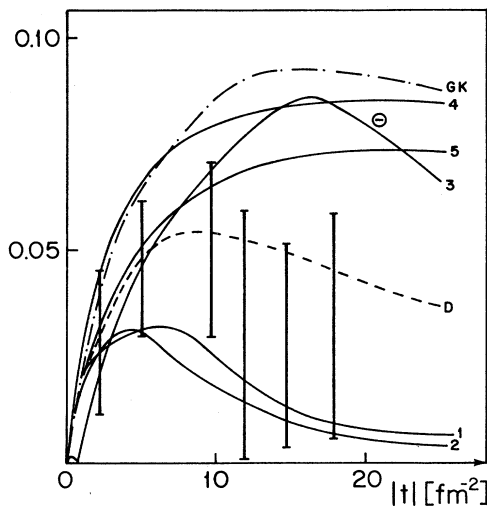


FIG. 2. Neutron electric form factor for various parameter sets. For notation see Fig. 1. Set 5 is defined by  $5 \equiv \{0.4, 1.9, -1.0\}$ . The empirical dipole fit ( $D$ ) as well as the semiphenomenological parametrization of Gari and Krümpelmann (GK) (Ref. 19) are also shown. The data are extracted from the paper of Galster *et al.* (Ref. 41) using the deuteron model of Lomon and Feshbach (Ref. 42).

NORMALIZED PROTON MAGNETIC FF  $G_M^p(t)/G_M^p(0)$

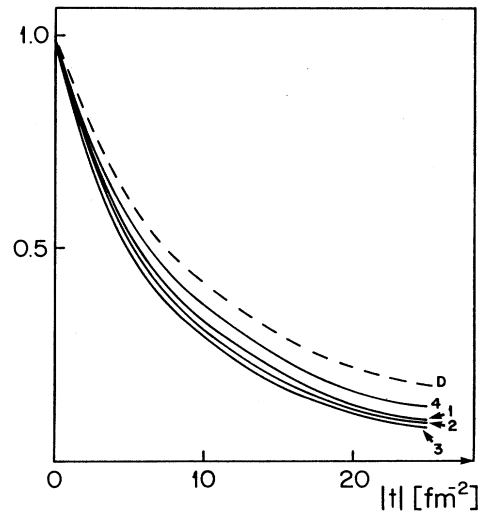


FIG. 3. Normalized proton magnetic form factor  $G_M^p(t)/G_M^p(0)$ . For notation, see Fig. 1.

nucleon and discuss some issues related to the Goldberger-Treiman relation. The axial form factor is related to the matrix element of the nucleon axial-vector current  $A_a^\mu(x)$  in the Breit frame via<sup>6</sup>

$$\begin{aligned} & \left\langle N_f \left[ \frac{\mathbf{q}}{2} \right] \middle| \mathbf{A}_a(0) \middle| N_i \left[ \frac{-\mathbf{q}}{2} \right] \right\rangle \\ &= \chi_f^\dagger \left[ \frac{E}{M_N} G_A(t) \sigma_L + \left[ G_A(t) + \frac{t}{4M_N^2} G_p(t) \right] \sigma_L \right] \frac{\tau_a}{2} \chi_i \end{aligned} \quad (3.25)$$

NORMALIZED NEUTRON MAGNETIC FF  $G_M^n(t)/G_M^n(0)$

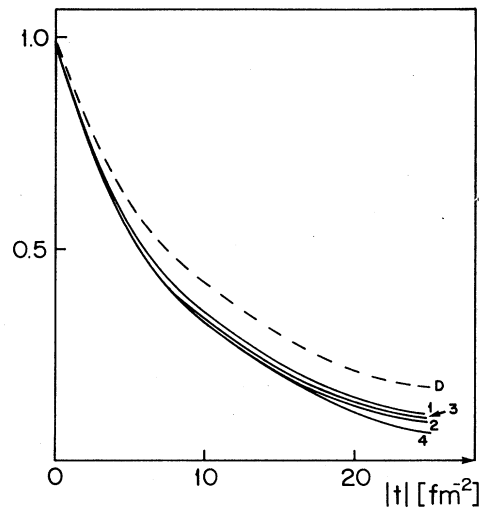


FIG. 4. Normalized neutron magnetic form factor  $G_M^n(t)/G_M^n(0)$ . For notation see Fig. 1. Notice that curves 2 and 3 are identical within the accuracy of the figure for  $|t| \leq 10 \text{ fm}^{-2}$ ; the same holds for 4 and 2 for  $|t| \leq 15 \text{ fm}^{-2}$ .

with  $t = -\mathbf{q}^2$ ,  $\sigma_1 = \sigma - \hat{q}(\sigma \cdot \hat{q})$ ,  $\sigma_L = \hat{q}(\sigma \cdot \hat{q})$ , and  $E = (\mathbf{q}^2/4 + M_N^2)^{1/2}$ . The induced pseudoscalar form factor  $G_p(t)$  is related via PCAC to the strong  $\pi N$  form factor  $G_{\pi NN}(t)$  and is discussed in some detail in Appendix C.

$G_A(\mathbf{q}^2)$  expressed in terms of the radial functions  $A_1$  and  $A_2$  reads

$$G_A(\mathbf{q}^2) = -\frac{8\pi}{3} \frac{M_N}{(M_N^2 + \mathbf{q}^2/4)^{1/2}} \times \int_0^\infty \left[ r^2 j_0(qr) A_1(r) + r^2 \frac{j_1(qr)}{qr} A_2(r) \right] dr. \quad (3.26)$$

Before presenting results, let us mention one pertinent difference to the complete model. There, the Bardeen-subtracted anomalous action was used which breaks chiral symmetry and leads to a violation of the Goldberger-Treiman relation of the order of 15% in the zero pion mass limit. In the model presented here, we have exact PCAC,

$$\partial_\mu A^{\mu,a}(x) = m_\pi^2 f_\pi \pi^a(x), \quad (3.27)$$

which leads to the Goldberger-Treiman relation (GTR)

$$G_{\pi NN}(0) = \frac{M_N}{f_\pi} G_A(0). \quad (3.28)$$

$G_{\pi NN}(0) \equiv g_{\pi NN}$  is the strong pion-nucleon coupling constant at  $t=0$  which will be evaluated in the following section. The GTR (3.28) gives a good check on the numerical accuracy. Furthermore, the pion-nucleon  $\Sigma$  term receives its only contribution from the chiral-symmetry-breaking pion mass term, i.e.,

$$\Sigma_{\pi N} = 4\pi f_\pi^2 m_\pi^2 \int_0^\infty r^2 (1 - \cos F) dr, \quad (3.29)$$

in contrast with the "complete model," where part of the anomalous action also contributes to  $\Sigma_{\pi N}$ .

In Table IV we summarize our results for the axial-vector coupling  $g_A = G_A(0)$ , the nucleon axial radius  $\langle r_A^2 \rangle^{1/2}$  and the  $\pi N \Sigma$  term for the parameter sets discussed before. In Fig. 5, we show the normalized axial form factor up to momentum transfer  $|t| \lesssim 25 \text{ fm}^{-2}$  in comparison with some data and the recent dipole fit of

NORMALIZED AXIAL FORM FACTOR  $G_A(\mathbf{q}^2)$

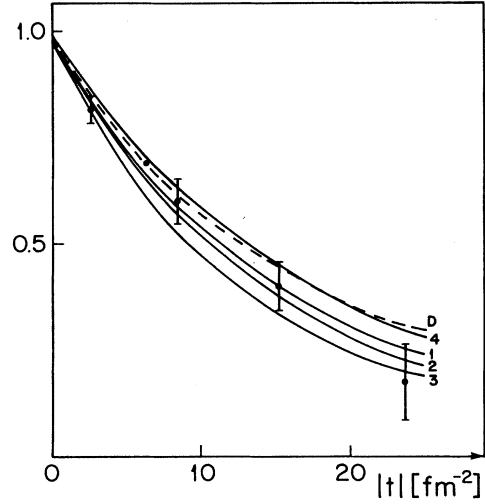


FIG. 5. Normalized axial form factor  $G_A(t)/G_A(0)$ . For notation see Fig. 1.  $D$  denotes the empirical dipole fit of Ahrens *et al.* (Ref. 20) with  $M_A = 1.09 \text{ MeV}$ .

Ahrens *et al.*<sup>20</sup> with  $M_A = 1.09 \text{ GeV}$ . For the central values, the form factor follows closely the dipole fit, somewhat different from the complete model. The axial-vector coupling constant  $g_A$  is close to one for the preferred set of values  $\bar{h} = 0.4$ ,  $\bar{g}_{\nu\nu\phi} = 1.9$ , and  $\kappa = +1$ . The  $\pi\rho\omega$  correlations are the reason for this enhancement of  $g_A$  as compared to the conventional Skyrme model. For the whole range of parameters with  $\kappa$  positive, the axial charge radius comes out reasonably close to the empirical value, and the  $\Sigma$  term is generally too small. This is, however, an expected result since we are dealing with the U(2) reduction of the Lagrangian. In a somewhat simplified SU(3) model, Blaizot, Rho, and Scoccola<sup>21</sup> have shown that the effect of strangeness is large enough to accommodate a  $\Sigma$  term of  $\sim 60 \text{ MeV}$ . For negative  $\kappa$ ,  $g_A$  tends to decrease drastically and the  $\Sigma$  term tends to become too large as can be read off from Table IV.

TABLE IV. Axial-vector properties of the nucleon. The axial-vector coupling  $g_A$ , the axial charge radius  $r_A$ , and the  $\pi N \Sigma$  term are given together with the results of the "complete" model and the empirical values (Refs. 20 and 31). The numbers for the complete model in parentheses refer to an alternative evaluation in Ref. 3.

$(\bar{h}, \bar{g}_{\nu\nu\phi}, \kappa)$	$g_A$	$r_A$ (fm)	$\Sigma_{\pi N}$ (MeV)
(+0.7, +2.2, 0.0)	0.53	0.59	18.5
(+0.4, +1.9, 0.0)	0.76	0.64	31.6
(+0.4, +1.9, +1.0)	0.91	0.66	41.6
(+0.4, +1.9, -1.0)	0.32	0.56	83.8
(-0.15, +1.3, 0.0)	1.38	0.71	76.7
Complete model	0.99 (0.91)	0.62	$\sim 200$ (156)
Expt.	$1.259 \pm 0.009$	$0.63 \pm 0.03$	$60 \pm 10$

Performing a spectral analysis of the axial form factor as outlined in Ref. 22,

$$G_A(t) = \frac{1}{\pi} \int_{9m_\pi^2}^{\infty} \frac{\text{Im}G_A(t')}{t'-t} dt', \quad (3.30)$$

we find that the spectral function is broadly peaked around  $t'=(0.9 \text{ GeV})^2$ , close to the result calculated in the complete model and not far from the axial-vector meson mass  $m(A_1)=(1056 \pm 35) \text{ MeV}$  as has been found recently in  $\tau \rightarrow A_1 + \text{neutrino}$  decays.<sup>23</sup> In summary, we can say that the axial properties of nucleons as described by the model presented here and for the preferred choice of parameters is similar in quality to the one quoted for the complete model. The model discussed here, however, is manifestly chiral invariant and leads to the Goldberger-Treiman relation resulting from exact PCAC.

#### D. Strong meson-nucleon form factors

The strong meson-nucleon vertex functions (the pion-nucleon form factor, the Dirac and Pauli form factors related to the  $\rho$  and  $\omega$  meson-nucleon couplings) give further insight into the structure of nucleons as solitons. They can be related to the *ad hoc* form factors used in boson exchange models of the nuclear force<sup>24</sup> and to dispersion theoretical approaches based on  $NN \rightarrow n\pi$  helicity amplitudes.<sup>25</sup>

First, let us consider the  $\pi NN$  form factor  $G_{\pi NN}(t)$  defined by

$$\langle N(p') | J_\pi^a(0) | N(p) \rangle = G_{\pi NN}(t) \bar{u}(p') i \gamma_5 \tau^a u(p) \quad (3.31)$$

with  $t=(p'_\mu - p_\mu)^2$  the invariant squared four-momentum transfer. The right-hand side of (3.31) can be related to the Fourier transform of the static source distribution of the pion field  $\varphi^a(\mathbf{r})$ . The latter is given by the field equation

$$(\nabla^2 - m_\pi^2) \varphi^a(\mathbf{r}) = J_\pi^a(\mathbf{r}), \quad (3.32)$$

where  $J_\pi^a(\mathbf{r})$  can be connected to the right-hand side of Eq. (6.6a) in I. Since the pion field is given by  $\varphi^a(\mathbf{r}) = (f_\pi/3) \boldsymbol{\sigma} \cdot \hat{\mathbf{r}} \tau^a \sin F(r)$ , the  $\pi NN$  form factor becomes

$$\begin{aligned} G_{\pi NN}(t) &= G_{\pi NN}(-\mathbf{q}^2) \\ &= \frac{8\pi}{3} M_N f_\pi m_\pi^2 \int_0^\infty r^2 \frac{j_1(qr)}{q} \sin F(r) dr. \end{aligned} \quad (3.33)$$

The pion-nucleon coupling constant at  $t=0$ ,  $G_{\pi NN}(0)$  follows to be

$$\begin{aligned} G_{\pi NN}(0) &\equiv g_{\pi NN} \\ &= \frac{8\pi}{9} M_N f_\pi m_\pi^2 \int_0^\infty r^3 \sin F(r) dr \end{aligned} \quad (3.34)$$

and it is related to the axial-vector coupling  $g_A$  via the GTR (3.28).

The vector-meson-nucleon form factors follow in a similar way from Fourier transform over the source functions  $J_\mu^a(\mathbf{r})$  via

$$(\nabla^2 - m_\rho^2) \rho_\mu^a(\mathbf{r}) = J_\mu^a(\mathbf{r}), \quad (3.35)$$

$$(\nabla^2 - m_\omega^2) \omega_\mu(\mathbf{r}) = J_\mu^0(\mathbf{r}) \quad (3.36)$$

with  $a=0$  for the isoscalar  $\omega$  meson and  $a=1,2,3$  for the isovector  $\rho$  meson. The corresponding Dirac and Pauli form factors  $F_1(t)$  and  $F_2(t)$  follow as

$$\begin{aligned} \langle N(p') | J_\mu^a(0) | N(p) \rangle \\ = \bar{u}(p') \left[ F_1^{(j)}(t) \gamma_\mu + \frac{i}{2M_N} F_2^{(j)}(t) \sigma_{\mu\nu} q^\nu \right] \tau^a u(p) \end{aligned} \quad (3.37)$$

( $j = \rho$  or  $\omega$ ) with  $\tau^0 = \mathbb{1}$  for the  $\omega$  and  $\tau^a$  ( $a=1,2,3$ ) for the  $\rho$ . We define vector and tensor couplings  $g_V$  and  $g_T$  by the values of  $F_1(t)$  and  $F_2(t)$  at  $t=0$  (notice that usually one defines  $g_V$  and  $g_T$  at the respective meson poles). For convenience, we also introduce the ‘‘electric’’ and ‘‘magnetic’’ vector-meson-nucleon form factors

$$\begin{aligned} G_E^{\rho,\omega}(t) &= F_1^{\rho,\omega}(t) + \frac{t}{4M_N^2} F_2^{\rho,\omega}(t), \\ G_M^{\rho,\omega}(t) &= F_1^{\rho,\omega}(t) + F_2^{\rho,\omega}(t), \end{aligned} \quad (3.38)$$

which in the Breit frame are identified with the Fourier transforms of the time and space components of the source  $J_\mu^a(\mathbf{r})$ . Therefore, we immediately have ( $m_\rho = m_\omega = m$ )

$$G_E^{\rho}(q^2) = \frac{2\pi}{\theta g} (q^2 + m^2) \int_0^\infty r^2 j_0(qr) [\xi_1(r) + \frac{1}{3} \xi_2(r)] dr, \quad (3.39a)$$

$$G_M^{\rho}(q^2) = -\frac{8\pi}{3g} M_N (q^2 + m^2) \int_0^\infty r^2 \frac{j_1(qr)}{qr} G(r) dr, \quad (3.39b)$$

$$G_E^{\omega}(q^2) = -4\pi (q^2 + m^2) \int_0^\infty r^2 j_0(qr) \omega(r) dr, \quad (3.39c)$$

$$G_M^{\omega}(q^2) = -2\pi \frac{M_N}{\theta} (q^2 + m^2) \int_0^\infty r^2 \frac{j_1(qr)}{qr} \phi(r) dr. \quad (3.39d)$$

Of course, we also have an  $\eta NN$  form factor. Here, we will set  $\eta(r)=0$  throughout and discuss the effects of the  $\eta$  together with  $G_{\eta NN}(q^2)$  in a later section.

Having set out the basic formalism let us now present the pertinent results. The normalized pion-nucleon form factor  $G_{\pi NN}(t)$  is shown in Fig. 6 for  $|t| \leq 25 \text{ fm}^{-2}$  together with a monopole with a cutoff  $\Lambda = 1 \text{ GeV}$  for the four sets of parameters defined before. At small  $t$ ,  $G_{\pi NN}(t)$  falls off like a monopole, for momentum transfer  $\gtrsim 10 \text{ fm}^{-1}$  it falls off somewhat faster. The pion-nucleon coupling constant defined at  $t=0$  is given in Table V. We see that for the central choice of parameters  $g_{\pi NN}$  is close to the empirical value, very similar to the complete model. The violation of PCAC together with the large value of  $\Sigma_{\pi N}$  (cf. Table IV) certainly constitute the most severe limitations of the complete model. For the vector-meson-nucleon form factors it is first important to notice

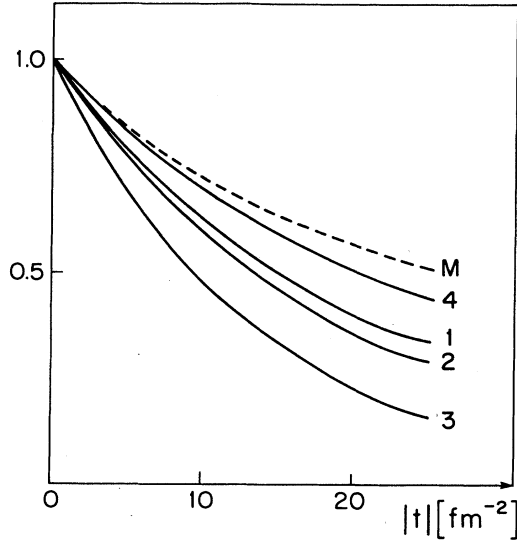


FIG. 6. Normalized strong pion-nucleon form factor. For notation, see Fig. 1.  $M$  denotes a monopole with a cutoff  $\Lambda=1.0$  GeV.

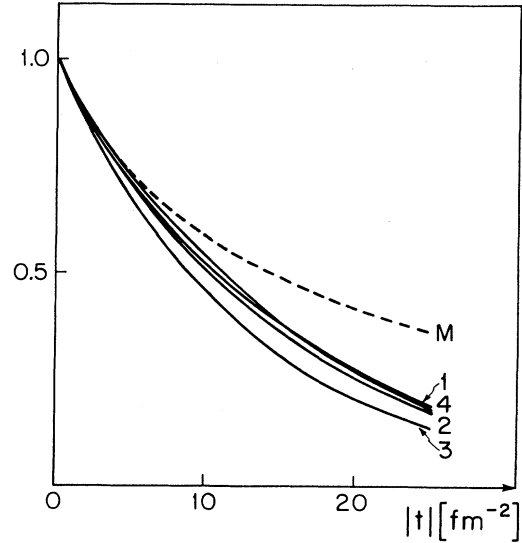


FIG. 7. Normalized strong  $\omega$ -meson-nucleon vector form factor  $F_1^\omega(t)$ . For notation see Fig. 1.  $M$  denotes a monopole with cutoff  $\Lambda=0.75$  GeV.

that the relative strengths of vector and tensor couplings follow the general systematics required by  $NN$ -interaction phenomenology: the  $\omega$ -meson-nucleon vertex is dominated by the vector coupling, whereas the  $\rho$ -meson-nucleon vertex is dominated by the tensor coupling. This is made explicit in Table V where the anomalous magnetic couplings for the  $\rho$  and the  $\omega$  are given, respectively. These are defined via  $\kappa_j = F_2^{(j)}(t=0)/F_1^{(j)}(t=0)$ . The respective form factors  $F_1^{(\omega)}(t)$  and  $F_2^{(\rho)}(t)$  are shown in Figs. 7 and 8 for our usual sets of parameters. It is interesting to note that  $\kappa_\omega = -0.1 \rightarrow -0.2$  for the whole parameter range, close to the empirical anomalous isoscalar moment of the nucleon,  $\kappa_s = -0.12$ . For the  $\rho$  meson, the situation is different. For the central choice of parameters, we have  $\kappa_\rho = 5.01$  ( $\kappa=0$ ) and  $\kappa_\rho = 5.62$  ( $\kappa=+1$ ), close to the empirical value  $\kappa_\rho \simeq 6.1$  (Ref. 26). Within the range of parameters,  $\kappa_\rho$  is rather strongly dependent on  $\gamma_1$  and  $\gamma_2$ . This can also be seen

from Fig. 9, in which we show  $\Lambda_\pi$ ,  $\Lambda_\rho$ ,  $\Lambda_\omega$ ,  $\kappa_\rho$ , and  $\kappa_\omega$  for the allowed range of  $\tilde{g}_{VV\phi}$  and  $\tilde{h}$  with  $\kappa=0$ . [The cutoffs  $\Lambda_\rho$  and  $\Lambda_\omega$  are defined via the dominant form factors  $F_2^\rho(t)$  and  $F_1^\omega(t)$ .]  $\Lambda_\omega$  is relatively stable, around 750 MeV (somewhat smaller than in the complete model).  $\Lambda_\pi$  and  $\Lambda_\rho$  are somewhat dependent on the  $\omega$ - $\phi$ -mixing angle, we find  $0.7 \leq \Lambda_\pi \leq 1.0$  GeV and  $0.7 \leq \Lambda_\rho \leq 1.2$  GeV. We should again stress that the results for the central choice of  $\tilde{g}_{VV\phi}$  and  $\tilde{h}$  together with  $\kappa=+1$  are very similar to the complete model. In contrast, choosing  $\kappa=-1.0$ , the strong meson-nucleon form factors cannot be described satisfactorily within our model.

Following the procedure outlined in Ref. 22, we have also performed a spectral decomposition of the pion-nucleon vertex function, which has a peak around  $\sqrt{t} = 7m_\pi$  for the central choice of parameters. This is consistent with dispersion-theoretical analyses<sup>25</sup> which point out the importance of  $\pi\rho$  intermediate states on top

TABLE V. Strong meson-nucleon vertex functions. The pion-nucleon coupling constant  $g_{\pi NN} = G_{\pi NN}(0)$ , the cutoffs  $\Lambda_\pi$ ,  $\Lambda_\rho$ ,  $\Lambda_\omega$ , and the anomalous magnetic couplings  $\kappa_\rho$  and  $\kappa_\omega$  are given. The cutoffs  $\Lambda_M$  are determined from fitting the form factors  $G_{\pi NN}(t)$ ,  $F_1^\omega(t)$ , and  $F_2^\rho(t)$  to monopoles at small  $t$ .  $\kappa_\rho$  and  $\kappa_\omega$  are defined at  $t=0$ , the empirical values are taken from Refs. 24 and 32. Empirical values in parentheses are from the OBE potential (Ref. 24). The results of the complete model are also given.

$(\tilde{h}, \tilde{g}_{VV\phi}, \kappa)$	$g_{\pi NN}$	$\Lambda_\pi$ (GeV)	$\Lambda_\rho$ (GeV)	$\Lambda_\omega$ (GeV)	$\kappa_\rho$	$\kappa_\omega$
(+0.7, +2.2, 0.0)	7.89	1.017	1.215	0.780	2.92	-0.12
(+0.4, +1.9, 0.0)	12.51	0.881	0.966	0.755	5.02	-0.19
(+0.4, +1.9, +1.0)	15.23	0.830	0.884	0.734	5.62	-0.29
(+0.4, +1.9, -1.0)	5.27	1.140	1.543	0.902	2.76	-0.27
(-0.15, +1.3, 0.0)	27.67	0.698	0.726	0.680	12.34	-0.21
Complete model	14.05	0.860	0.95	0.86	4.36	-0.07
Expt.	13.45	0.890 (1.3)	(1.4)	(1.5)	6.1	-0.12

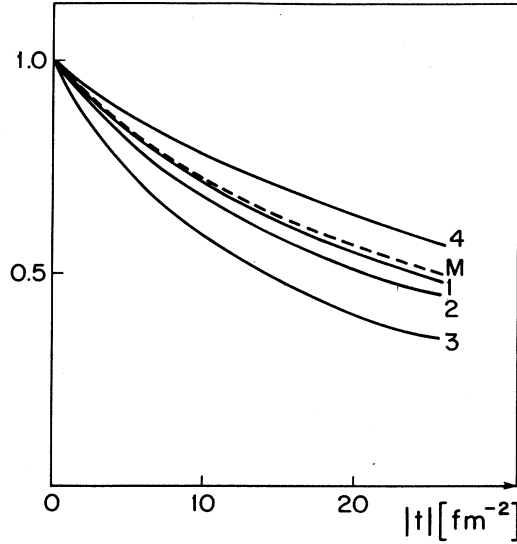


FIG. 8. Normalized strong  $\rho$ -meson-nucleon tensor form factor  $F_2^\rho(t)$ . For notation, see Fig. 1.  $M$  denotes a monopole with a cutoff  $\Lambda=1.0$  GeV.

of a broad  $3\pi$  continuum. To summarize this section, we can say that the predicted  $\pi NN$  form factor agrees well with the phenomenological analysis, whereas the sizes of the  $\omega$  and  $\rho$  nucleon vertex measured by  $r_{\rho,\omega}=\sqrt{6}/\Lambda_{\rho,\omega}$  are somewhat larger than the ones commonly used in one-boson-exchange potentials.

### E. Effects of the $\eta$ meson

Up to now, we had set  $\eta(r)=0$  and therefore neglected the effects of  $\eta$  on the static properties and the strong

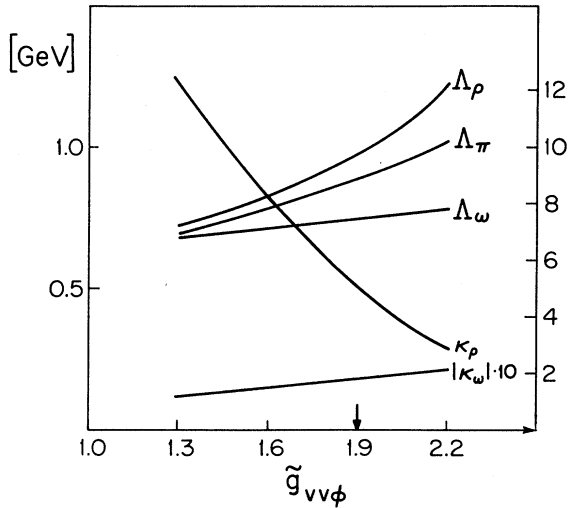


FIG. 9. Strong meson-nucleon vertices. The cutoffs  $\Lambda_\pi$ ,  $\Lambda_\rho$ , and  $\Lambda_\omega$  (left-hand scale) are shown as a function of  $\tilde{g}_{\nu\nu\phi}$  together with  $\kappa=0$ . The arrow denotes the central values of  $\tilde{g}_{\nu\nu\phi}$  and  $\bar{h}$ . Also shown are the vector to tensor ratios  $\kappa_i=F_2^i(0)/F_1^i(0)$  ( $i=\rho,\omega$ ) (right-hand scale). Notice that only  $\kappa_\rho$  depends strongly on  $\tilde{g}_{\nu\nu\phi}$ .

form factors. In I we had already argued that these effects should be small, which should be expected both from the weak influence of the  $\eta$  on the  $NV$  force and from the fact that it only couples to the soliton after the semiclassical quantization. We will demonstrate that our arguments in I were indeed justified and, furthermore, we will discuss the strong  $\eta NN$  form factor and its relation to one-boson-exchange models. Before proceeding, we should point out that the field “ $\eta$ ” we are using is not quite the physical one but is related to the physical  $\eta$  and  $\eta'$  fields by

$$\begin{aligned} \text{“}\eta\text{”} &= \left[ \frac{c}{\sqrt{3}} - \frac{2s}{\sqrt{6}} \right] \eta + \left[ \frac{s}{\sqrt{3}} + \frac{2c}{\sqrt{6}} \right] \eta' \\ &\approx \frac{4}{5} \eta + \frac{3}{5} \eta', \end{aligned} \quad (3.40)$$

where  $c=\cos\theta_p$ ,  $s=\sin\theta_p$  and the pseudoscalar mixing angle  $\theta_p$  was taken as  $-18^\circ$ . A more accurate treatment of the  $\eta$  would require us to also include the strange particles in our calculation. For definiteness we will consider the mass of “ $\eta$ ” to be 549 MeV.

Let us first discuss the contribution of the  $\eta$  to the moment of inertia, i.e., the nucleon and the  $\Delta(1232)$  mass. For orientation, we will consider first a “minimal” model<sup>27</sup> with  $\gamma_1 \neq 0$ ,  $\gamma_2 = \gamma_3 = 0$ . In particular, we have  $g_\omega = (3g/2)$ , i.e.,  $\bar{h} = -0.4194$ . In Fig. 10 the  $\eta$  profile is

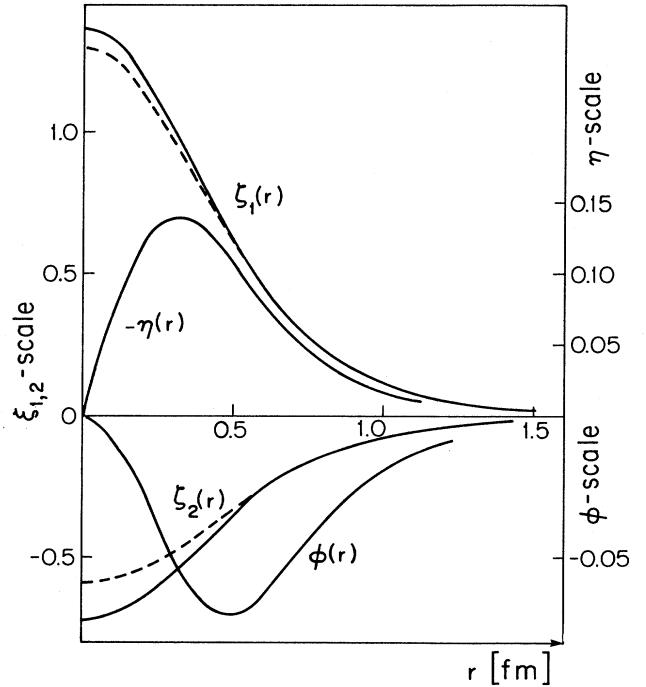


FIG. 10. Vector-meson excitations in the presence of the  $\eta$  meson. The solid lines give the profiles  $\xi_1(r)$ ,  $\xi_2(r)$ , and  $\phi(r)$  [see Eqs. (3.4)] for a minimal model with  $\gamma_1 = -0.4194$  ( $g_\omega = 8.78$ ) and  $\gamma_2 = \gamma_3 = 0$ . The dashed lines give the same profiles in the presence of the  $\eta$  [solid line labeled “ $-\eta(r)$ ”] for  $m_\eta = 549$  MeV.

shown as well as the profiles of the vector-meson excitations  $\zeta_1$ ,  $\zeta_2$ , and  $\Phi$ . The  $\eta$  profile is small throughout, and the vector-meson profiles are only mildly affected. The moment of inertia changes from  $\theta=0.824$  fm [for  $\eta(r)=0$ ] to  $\theta=0.834$  fm. The direct contribution from the  $\eta$  is  $\theta_\eta=4\pi\int_0^\infty\Lambda_\eta dr\simeq 0.03$  fm. This amounts to a decrease of  $\sim 4$  MeV in the  $N\Delta$  mass splitting, which is only a very small effect. Allowing for  $\gamma_2$  and  $\gamma_3$  being nonzero, this trend persists. For the central values of the parameters, the nucleon mass is decreased by  $\sim 5$  MeV, and over the whole range of parameters, the  $\eta$  decreases the moment of inertia by a few percent. The effect of the  $\eta$  on the electromagnetic properties in Sec. III B is similarly small.

As in the previous section, the equation of motion for the  $\eta$ ,

$$(\nabla^2 - m_\eta^2)\eta(\mathbf{r}) = J_\eta(\mathbf{r}), \quad (3.41)$$

can be used to define the strong  $\eta NN$  form factor as the Fourier transform over the source function  $J_\eta(\mathbf{r})$ . One easily finds

$$G_{\eta NN}(\mathbf{q}^2) = -\frac{2\pi}{\theta} M_N (q^2 + m_\eta^2) \int_0^\infty r^3 \frac{j_1(qr)}{qr} \eta(r) dr \quad (3.42)$$

and the  $\eta NN$  coupling constant at  $\mathbf{q}^2=0$  is given by

$$g_{\eta NN} = -\frac{2\pi}{3\theta} M_N m_\eta^2 \int_0^\infty r^3 \eta(r) dr. \quad (3.43)$$

For the minimal model,  $G_{\eta NN}(\mathbf{q}^2)$  is shown in Fig. 11 together with a monopole factor with a cutoff of  $\approx 1$  GeV. We find  $g_{\eta NN}=1.61$ , somewhat small compared to the

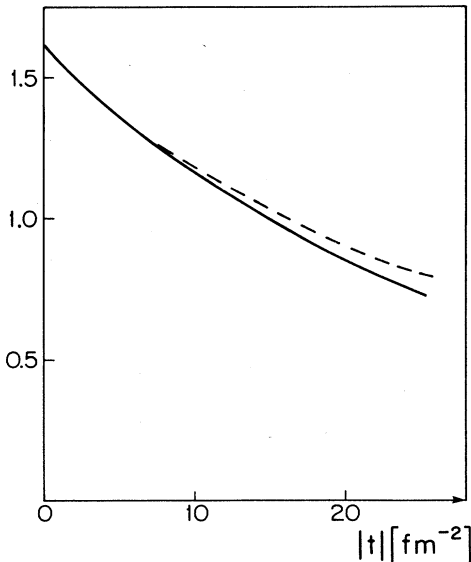


FIG. 11. Strong  $\eta NN$  form factor for a minimal model. For notation see Fig. 10.  $M$  denotes a monopole with a cutoff  $\Lambda=1.0$  GeV.

SU(3) value  $g_{\eta NN}=\sqrt{3/25}g_{\pi NN}$  (Ref. 28) and the one-boson-exchange-potential (OBEP) value  $g_{\eta NN}^{\text{OBE}}=6.86$  (Ref. 24). The form factor can be fitted to a monopole at small  $t$  with a cutoff  $\tilde{\Lambda}_\eta=1.08$  GeV, as compared to  $\tilde{\Lambda}_\eta=1.5$  GeV used in Ref. 24. For the central choice of parameters, the  $\eta$  profile is somewhat more pronounced and we find  $g_{\eta NN}=5.60$  and  $\tilde{\Lambda}_\eta=0.84$  GeV. It might be interesting to note that some versions of the Bonn potential<sup>24</sup> do not include the  $\eta$ , while others do. This is another manifestation of the fact that the  $\eta$  plays only a minor role in the  $NV$  force, and should therefore have only mild effects on the soliton properties as we have demonstrated.

#### IV. SUMMARY AND OUTLOOK

It is generally believed that a suitable Lagrangian of pseudoscalars and vectors should provide a realistic testing ground for the notion that the nucleon is a solitonic excitation. Here, we have investigated in detail this conjecture within the framework of a Lagrangian set up in I. It has three coefficients which can be exclusively determined from strong interaction processes, plus an extra one when electromagnetism is carefully added. Two of the three strong-interaction constants have been determined in I. The remaining one could not be fixed from existing meson data, while a plausible range for its value was given in I from the study of some bulk properties of the soliton,  $\kappa \approx 1$ . We should stress that the freedom in adjusting  $\kappa$  did not enable us to solve the problem of the too high mass of the nucleon and the  $\Delta(1232)$ .

Here, we went one step further. We performed an adiabatic quantization of the soliton and calculated a variety of its properties, with particular emphasis on the electromagnetic currents. First, we determined the new constant  $d_1/h$  from the  $\omega \rightarrow \pi^0 \gamma$  decay to be

$$\frac{d_1}{h} = \frac{R}{2} + \frac{\tilde{g}_{VV\phi}}{4g^2} = \pm 0.02 + \frac{\tilde{g}_{VV\phi}}{4g^2} \quad (4.1)$$

with  $R = \pm 0.04$ . All currents were calculated in a direct manner and it was found that new contributions to both vectors and axial-vector currents involving  $d_1$  emerged. Although we did not assume vector-meson dominance, the electromagnetic radii, magnetic moments, and form factors turn out to be of similar quality to the ones of the complete model (Ref. 6). Similar statements can be made for the axial-vector coupling constant and the axial form factor. The model presented here predicts an axial form factor which follows closely the empirical dipole fit of Ahrends *et al.*<sup>20</sup> In contrast with the complete model, our Lagrangian embodies exact PCAC, therefore, overcoming the most severe limitation of models making use of the Bardeen-subtracted Wess-Zumino action. We have also demonstrated that the model considered here makes contact with semiphenomenological one-boson-exchange models of the nucleon-nucleon force. It predicts coupling constants and form factors familiar from the phenomenology of the  $NN$  interaction. In particular, the  $\rho NN$  interaction has a dominant tensor coupling, whereas the  $\omega NN$  interaction is governed by its vector coupling.

Through the adiabatic quantization the isoscalar-

pseudoscalar  $\eta$  gives a contribution to the nucleon mass and its other properties. We have justified our conjecture in I that these effects will be small. For example, the  $\eta$  brings down the nucleon mass by a few MeV, the influence of the  $\eta$  on the other properties of the nucleon is similarly small.

In light of the recent discussion concerning the spin content of the proton<sup>29</sup> and the admixture of strange operators in the proton's wave function,<sup>30</sup> it appears to be of utmost importance to perform a full U(3) treatment of the Lagrangian considered here. Research along these lines is underway.

#### ACKNOWLEDGMENTS

This work was supported in part by funds provided by the U.S. Department of Energy (DOE) under Contract

Nos. DE-AC02-76ER03069 and DE-FG02-85ER40231, and in part by the Deutsche Forschungsgemeinschaft.

#### APPENDIX A: EQUATIONS OF MOTION FOR THE MESON EXCITATIONS AND THE REDUCED MOMENT OF INERTIA

Here, we wish to present the coupled equations of motion for the vector-meson excitations  $\xi_1(r)$ ,  $\xi_2(r)$ , and  $\phi(r)$  defined in (3.2) as well as the  $\eta$ -profile  $\eta(r)$  defined in (3.3). These follow by extremizing the moment-of-inertia functional (3.5). Furthermore, these equations of motion can be used to bring the moment of inertia functional into a much shorter, the so-called "reduced form." This reduced form of  $\Lambda(\Lambda_{\text{red}})$  can be used as an excellent check on the numerical solutions of the coupled equations of motion, which read

$$\begin{aligned} \xi_1'' = & -\frac{2}{r}\xi_1 + m^2\xi_1 - 4f_\pi^2 g^2 \sin^2\left(\frac{F}{2}\right) + \frac{1}{r^2}[G^2(\xi_1 - 1) - 2(G+1)\xi_2] \\ & - \frac{\gamma_2 g^2}{2r^2}\phi'\sin F - \frac{\gamma_3 g^2}{2r^2}\phi F'(G+1-\cos F) + \frac{g}{2r^2 f_\pi}\eta\left[-\frac{\gamma_1}{3}F'\sin F + \gamma_2 G'\right], \end{aligned} \quad (\text{A1})$$

$$\begin{aligned} \xi_2'' = & -\frac{2}{r}\xi_2 + m^2\xi_2 + 4f_\pi^2 g^2 \sin^2\left(\frac{F}{2}\right) + \frac{1}{r^2}[G^2(\xi_1 - 1) + 2(G^2 + 3G + 3)\xi_2] \\ & + \frac{\gamma_2 g^2}{2r^2}(\phi'\sin F - 2\phi F') + \frac{\gamma_3 g^2}{2r^2}\phi F'(G+1-\cos F) \\ & + \frac{g}{2r^2 f_\pi}\eta\left[-\frac{\gamma_1}{3}\sin^2 F + \gamma_2[2G\cos F - (1-\cos F)^2] - 3\gamma_3(G+1-\cos F)^2\right] + \frac{g}{2r^2 f_\pi}\eta\left[\frac{\gamma_1}{3}F'\sin F - \gamma_2 G'\right], \end{aligned} \quad (\text{A2})$$

$$\begin{aligned} \phi'' = & \frac{2}{r^2}\phi + m^2\phi - 2\gamma_1 F'\sin^2 F + 2\gamma_2\{(G-\xi_1)F'\cos F + (G'-\xi_1')\sin F + F'[\xi_1 + \xi_2 - (1-\cos F)^2]\} \\ & - 2\gamma_3 F'[(1-\cos F)(G-\xi_1) + (1-\cos F)^2 - G\xi_1] - \frac{g\gamma_2\eta\omega'}{f_\pi}, \end{aligned} \quad (\text{A3})$$

$$\begin{aligned} \eta'' = & -\frac{2}{r}\eta' + \frac{2}{r^2}\eta + \bar{m}^2\eta + m_\pi^2\eta\cos F - \frac{2\gamma_1}{3gf_\pi r^2}[F'\sin 2F(\xi_1 + \xi_2) + (\xi_1' + \xi_2')\sin^2 F - 2F'\sin F(G + \xi_1)] \\ & - \frac{2\gamma_2}{gf_\pi r^2}\{2G'[G + \xi_1 - (\xi_1 + \xi_2)\cos F] + 2F'\sin F(\xi_1 + \xi_2)(G + 1 - \cos F) + (\xi_1' + \xi_2')[ (1 - \cos F)^2 - 2G\cos F]\} \\ & - \frac{6\gamma_3}{gf_\pi r^2}(G + 1 - \cos F)[2(G' + F'\sin F)(\xi_1 + \xi_2) + (G + 1 - \cos F)(\xi_1' + \xi_2')] - \frac{2\gamma_2 g}{f_\pi r^2}\phi\omega' \end{aligned} \quad (\text{A4})$$

subject to the boundary conditions

$$\xi_1'(0) = \xi_1'(\infty) = 0, \quad \xi_2'(0) = \xi_2'(\infty) = 0, \quad \phi(0) = \phi(\infty) = 0, \quad \eta(0) = \eta(\infty) = 0, \quad (\text{A5})$$

and the constraint (at  $r=0$ )

$$2\xi_1(0) + \xi_2(0) = 2. \quad (\text{A6})$$

One can now use the equations of motion (A1)–(A4) to reduce the lengthy expression of the moment of inertia (3.5). One finds that terms bilinear in the excitations and their derivatives drop out, terms linear in the excitations receive a factor ( $\frac{1}{2}$ ) and terms independent of the excitations remain unchanged. Therefore, the reduced form of the moment of inertia reads

$$\begin{aligned} \Lambda_{\text{red}} = & \frac{2}{3} r^2 f_\pi^2 \left[ \sin^2 F + 8 \sin^4 \left[ \frac{F}{2} \right] - 4 \sin^2 \left[ \frac{F}{2} \right] \xi_1 \right] + \frac{2G^2}{3g^2} (2 - 2\xi_1 - \xi_2) + \frac{\gamma_1}{3} \phi F' \sin^2 F \\ & + \frac{\gamma_2}{6} (\phi' \sin F (G + 2 - 2\cos F) + \phi \{ F' [2 - (G + 2)\cos F + 2 \sin^2 F] - G' \sin F \}) + \frac{\gamma_3}{3} (1 - \cos F) \phi F' (G + 1 - \cos F) \\ & - \frac{\gamma_1}{9g f_\pi} \eta F' G \sin F - \frac{\gamma_2}{6g f_\pi} \{ \eta' G (G + 1 - \cos F) + \frac{\eta}{f_\pi} [G' (1 - \cos F) + F' G \sin F] \}. \end{aligned}$$

To have a check on the numerical solutions to the coupled equations for  $\xi_1$ ,  $\xi_2$ ,  $\phi$ , and  $\eta$ , we demand  $|\Lambda/\Lambda_{\text{red}} - 1| < 10^{-5}$ . This together with (A6) serves as an excellent check on the numerical analysis.

### APPENDIX B: THE RADIAL FUNCTIONS

The radial functions  $R_i(r)$  as defined in (3.16) in the presence of the  $\eta$  meson are listed in this appendix (for simplicity we choose the abbreviations  $s = \sin F$  and  $c = \cos F$ ):

$$\begin{aligned} R_2(r) = & \frac{1}{12\theta r^2} \left[ -\frac{m^2 \phi}{g} + \left[ \frac{2\gamma_1}{g} - \frac{N_c}{2\pi^2} \right] F' s^2 - 4 \frac{d_1}{h} \left[ F' (\xi_1 + \xi_2) + \frac{d}{dr} [s(2 + G - \xi_1 - 2c)] \right] \right] \\ & + \frac{\gamma_2}{g} \{ 3F' s^2 + F' [(1 - c)^2 + (\xi_1 - G)c - \xi_1 - \xi_2] + s(\xi' - G') \} \\ & + \frac{2\gamma_3}{g} F' [(1 - c)(G - \xi_1) + (1 - c)^2 - G\xi_1] + \frac{g}{2} \left[ \frac{\gamma_2}{g} - 4 \frac{d_1}{h} \right] \frac{\eta}{f_\pi} \omega', \end{aligned} \quad (\text{B1})$$

$$\begin{aligned} R_3(r) = & \frac{1}{3\theta} \left[ f_\pi^2 \{ s^2 + \mu^2 [(1 + 2c)\xi_1 + \xi_2 - 2c(1 - c)] \} + \frac{1}{2} \gamma_1 F' \frac{\phi}{r^2} s^2 + \frac{1}{4} \frac{\gamma_2}{r^2} [3F' \phi s^2 - F' \phi + \phi' s (G + 1 - 2c) - G' \phi s] \right. \\ & - \frac{1}{4} (\gamma_2 + 2\gamma_3) F' \frac{\phi}{r^2} c (1 + G - c) - g \frac{d_1}{h} \frac{1}{r^2} \frac{d}{dr} (\phi s c) \\ & + \frac{1}{4g f_\pi r^2} \left[ \frac{N_c g}{12\pi^2} (2F' \eta s c + \eta' s^2) - \frac{\gamma_1}{3} [\eta' s^2 + 2\eta F' (G + 1)s] \right. \\ & \left. + \gamma_2 \{ \eta G' c + \eta' [(G + 1)c - 1] - \eta F' (G + 1)s \} \right. \\ & \left. - (\gamma_2 + 3\gamma_3) \eta' (1 + G - c)^2 - 4g \frac{d_1}{h} \frac{d}{dr} [\eta c (1 + G - c)] \right] \Bigg], \end{aligned} \quad (\text{B2})$$

$$\begin{aligned} R_4(r) = & \frac{1}{3r^2} \left[ f_\pi^2 [s^2 - 2\mu^2 c (1 + G - c)] + \gamma_1 \omega F' s^2 + \frac{1}{2} \gamma_2 [3\omega F' s^2 + \omega' s (1 + G - 2c) - \omega G' s - \omega F' c (1 + G - c)] \right. \\ & \left. - \gamma_3 \omega F' c (1 + G - c) + 2g \frac{d_1}{h} \left[ \omega F' - \frac{d}{dr} (\omega s c) \right] \right]. \end{aligned} \quad (\text{B3})$$

The terms proportional to  $N_c$  arise from the gauged WZ term  $\Gamma_{\text{WZ}}(U, B_L, B_R)$  in (3.11) of I. Of course, we have  $N_c = 3$ . Furthermore, the dimensionless constant  $\mu = m / (\sqrt{2} g f_\pi)$  is 1 if the KSFR relation is imposed.

### APPENDIX C:

#### THE INDUCED PSEUDOSCALAR FORM FACTOR

In the nucleon matrix element of the axial-vector current [Eq. (3.25)], we encountered the induced pseudoscalar form factor  $G_p(t)$ . Using PCAC, one can show that it is related to the axial form factor  $G_A(t)$  and the strong pion-nucleon form factor  $G_{\pi NN}(t)$  via

$$G_A(t) + \frac{t}{4M_N^2} G_p(t) = \frac{m_\pi^2 f_\pi}{M_N(m_\pi^2 - t)} G_{\pi NN}(t) \quad (\text{C1})$$

with  $t = -\mathbf{q}^2$  and  $M_N$  the nucleon mass. One can, alternatively,

evaluate  $G_p(t)$  directly from the matrix element (3.25) and finds

$$\begin{aligned} G_p(t) = & -\frac{32\pi M_N^2}{3t} \\ & \times \int_0^\infty \left[ r^2 j_0(qr) \left[ A_1(r) \left[ 1 - \frac{M_N}{E} \right] + A_2(r) \right] \right. \\ & \left. - \frac{r}{q} j_1(qr) A_2(r) \left[ 2 + \frac{M_N}{E} \right] \right] dr, \end{aligned} \quad (\text{C2})$$

where  $E = (M_N^2 + \mathbf{q}^2/4)^{1/2}$ . The radial functions  $A_1(r)$  and  $A_2(r)$  are given in (3.24). For small momentum transfer, the induced pseudoscalar form factor is dominated by the pion-pole term, which in turn leads to

TABLE VI. The induced pseudoscalar form factor  $G_p(t)$  in comparison to the pion-pole-dominance values for momentum transfers  $1 \text{ fm}^{-1} \leq \sqrt{-t} \leq 5 \text{ fm}^{-1}$ . The central values  $\bar{g}_{VV\phi} = +1.9$ ,  $\bar{h} = +0.4$ ,  $\kappa = 1.0$ ,  $R = -0.04$  together with the standard input  $f_\pi = 93.0 \text{ MeV}$ ,  $m_\pi = 138.0 \text{ MeV}$ , and  $g = 5.8545$  are used.

$\sqrt{-t} \text{ (fm}^{-1}\text{)}$	$G_p(t)$	$G_p^\pi(t)$
1	139.5	144.6
2	36.4	40.6
3	11.7	14.8
4	3.9	6.0
5	1.3	1.5

$$G_p^\pi(t) = \frac{4M_N f_\pi}{m_\pi^2 - t} g_{\pi NN}. \quad (\text{C3})$$

Experimentally, very little is known about the induced pseudoscalar form factor. It is measured at  $t = -m_\mu^2$  from the  $\mu$ -capture reaction  $\mu^- + p \rightarrow \nu_\mu + n$ <sup>33</sup>:

$$\frac{m_\mu}{2M_N} G_p(-m_\mu^2) \equiv g_p = (8.25 \pm 2.4). \quad (\text{C4})$$

In Table VI we summarize the pseudoscalar form factor  $G_p(t)$  as calculated from (C2) in comparison with the pion-pole dominated piece  $G_p^\pi(t)$ , as given in (C3) for the central values of the parameters together with  $\kappa = +1.0$ . At small momentum transfer, these values are of course identical, for  $|t| > 1 \text{ fm}^{-2}$  we see the expected deviations from pion-pole dominance. At the  $\mu$  pole, we find

$$g_p = \frac{m_\mu}{2M_N} G_p(-m_\mu^2) = 9.59 \quad (\text{C5})$$

in fair agreement with the empirical value (C4). To check the sensitivity of  $g_p$  versus parameter changes we have also calculated  $g_p$  for the edges of the allowed range for  $\bar{g}_{VV\phi}$  and  $\bar{h}$  (with  $\kappa = 0$  and  $R = -0.04$ ). We find

$$g_p = \begin{cases} 4.99 & \text{for } \bar{h} = +0.7, \bar{g}_{VV\phi} = +2.2 \\ 17.31 & \text{for } \bar{h} = -0.15, \bar{g}_{VV\phi} = +1.3 \end{cases} \quad (\text{C6})$$

which is similar to the parameter sensitivity of  $g_{\pi NN}$  exhibited in Table III. For comparison, in the complete model one finds  $g_p = 8.86$  (Ref. 34), which is not surprisingly close to the value with the central values and  $\kappa = 1.0$  [Eq. (C5)].

#### APPENDIX D: THE WEAK PION-NUCLEON VERTEX

In this appendix, we are going to calculate the parity-violating weak pion-nucleon vertex strength defined via

$$\mathcal{L}_{\pi NN}^{\text{PV}} = \frac{1}{2} G_\pi \bar{N} (\boldsymbol{\pi} \times \boldsymbol{\tau})_3 N \quad (\text{D1})$$

with  $N$  denoting a nucleon spinor and  $G_\pi$  the weak  $\pi N$  coupling strength to be calculated. We will essentially follow the work of Ref. 9 and omit any calculational detail here. To obtain the weak pion-nucleon amplitude,

TABLE VII. The weak pion-nucleon coupling constant  $\tilde{G}_\pi$  for various parameter sets with  $R = -0.04$ . We also give the results of the  $\gamma$  asymmetry in  $^{18}\text{F}$  together with the empirical data (Ref. 59) and results of the complete model.

$(\bar{h}, \bar{g}_{VV\phi}, \kappa)$	$\tilde{G}_\pi$	$ P_\gamma(^{18}\text{F}) $
(0.7, 2.2, 0)	$15.4 \times 10^{-8}$	$2.8 \times 10^{-4}$
(0.4, 1.9, 0)	$8.5 \times 10^{-8}$	$1.7 \times 10^{-4}$
(0.4, 1.9, +1)	$8.0 \times 10^{-8}$	$1.5 \times 10^{-4}$
(-0.15, 1.3, 0)	$15.2 \times 10^{-8}$	$2.8 \times 10^{-4}$
Complete model	$8.8 \times 10^{-8}$	$1.8 \times 10^{-4}$
Expt.	$< 3.4 \times 10^{-7}$	$(1.2 \pm 3.8) \times 10^{-4}$

one first has to construct an effective current  $\times$  current Hamiltonian starting from the standard model. Expressing the pertinent matrix elements via the soliton currents, we end up with (for a more thorough discussion, the interested reader should consult Ref. 9)

$$\begin{aligned} \tilde{G}_\pi &= G_\pi g_{\pi NN} / \sqrt{32} \\ &= 4\pi \sin^2 \theta_W G_F g_{\pi NN} \\ &\quad \times \int_0^\infty [r^2 R_1(r) R_3(r) - 2r^2 R_2(r) R_4(r)] dr, \end{aligned} \quad (\text{D2})$$

where we have introduced the commonly used definition of the weak pion-nucleon coupling strength.<sup>35</sup> We have also corrected for an incorrect normalization which appears in Ref. 9. Before presenting our results, let us mention that the  $\gamma$ -asymmetry data from  $^{18}\text{F}$  set a solid constraint on  $\tilde{G}_\pi$ , indeed one has<sup>36</sup>

$$\tilde{G}_\pi^{\text{exp}} < 3.6 \times 10^{-7}. \quad (\text{D3})$$

Our results are summarized in Table VII. Throughout this appendix, we will set  $\eta(r) = 0$  since the  $\eta$  terms have only mild influences on the current densities, and use  $R = -0.04$ . For our standard sets of parameters, we give the value of  $\tilde{G}_\pi$  together with the predicted  $\gamma$  asymmetry in  $^{18}\text{F}$ , which has been reported by Haxton,<sup>37,40</sup>

$$|P_\gamma(^{18}\text{F})| = (2.0 \pm 0.5) \times 10^{-3} \left[ \frac{\tilde{G}_\pi}{\tilde{G}_\pi^{\text{DDH}}} \right], \quad (\text{D4})$$

where  $\tilde{G}_\pi^{\text{DDH}} = 1.08 \times 10^{-6}$  is the quark-model estimate of Desplanques, Donoghue, and Holstein,<sup>38</sup> which is above the experimental limit (D3). We should point out that a recent quark-model calculation of Dubovik and Zenkin<sup>39</sup> tends to favor small values of  $\tilde{G}_\pi$ , typically close to the empirical limit. Our results are on the small end of the allowed values, and predict a  $\gamma$  asymmetry in  $^{18}\text{F}$  close to the empirical value. It is interesting to note that for the central values of  $\bar{g}_{VV\phi}$  and  $\bar{h}$  together with  $\kappa = 0$  or  $\kappa = +1.0$ , the result for  $\tilde{G}_\pi$  is within 10% of the result for the complete model.<sup>9</sup> Of course, the values for  $\tilde{G}_\pi$  obtained here should be considered as a lower bound.<sup>40-42</sup> In a  $U(3)$  treatment of our Lagrangian additional nonfactorizable diagrams will contribute to  $\tilde{G}_\pi$ . For a discussion on these points, we again refer the reader to Ref. 9.

- <sup>1</sup>P. Jain, R. Johnson, Ulf-G. Meissner, N. W. Park, and J. Schechter, *Phys. Rev. D* **37**, 3252 (1988), and references therein. Note that the vertical scale in Fig. 1 of this reference should be multiplied by 2. Also, in Fig. 2, the solid lower curve should be labeled  $-\omega(r)$  and the dashed lower curve should be labeled  $\omega(r)$ . Also see the remark after (2.12) of the present paper.
- <sup>2</sup>Ulf-G. Meissner, *Phys. Rep.* **161**, 213 (1988), and references therein.
- <sup>3</sup>B. Schwesinger, H. Weigel, G. Holzwarth, and A. Hayashi, *Phys. Rep.* (to be published), and references therein.
- <sup>4</sup>Ö. Kaymakçalan and J. Schechter, *Phys. Rev. D* **31**, 1109 (1985).
- <sup>5</sup>G. S. Adkins, C. R. Nappi, and E. Witten, *Nucl. Phys.* **B228**, 552 (1983).
- <sup>6</sup>Ulf-G. Meissner, N. Kaiser, and W. Weise, *Nucl. Phys.* **A466**, 685 (1987).
- <sup>7</sup>Ulf-G. Meissner and I. Zahed, *Z. Phys. A* **327**, 5 (1987); Ulf-G. Meissner and N. Kaiser, *Phys. Rev. D* **36**, 203 (1987).
- <sup>8</sup>M. Lacombe *et al.*, *Phys. Rev. D* **38**, 1491 (1988).
- <sup>9</sup>N. Kaiser and Ulf-G. Meissner, MIT Report No. CTP 1564, 1988 (unpublished); *Nucl. Phys.* **A489**, 671 (1988).
- <sup>10</sup>This value is above the critical coupling  $g_c = 4.8$  below which spontaneous parity violation might occur as recently discussed by Y. Igarashi, A. Kobayashi, H. Otsu, and S. Sawada, *Phys. Lett. B* **214**, 445 (1988).
- <sup>11</sup>K. Kawarabayashi and M. Suzuki, *Phys. Rev. Lett.* **16**, 255 (1966); Riazuddin and Fayyazuddin, *Phys. Rev.* **147**, 1071 (1966).
- <sup>12</sup>M. Bando, T. Kugo, and K. Yamawaki, *Nucl. Phys.* **B259**, 493 (1985); *Phys. Rep.* **164**, 217 (1988), and references therein.
- <sup>13</sup>J. Schechter, *Phys. Rev. D* **34**, 868 (1986); see also Ulf-G. Meissner and I. Zahed in Ref. 7.
- <sup>14</sup>E. Witten, *Nucl. Phys.* **B223**, 442 (1983); **B223**, 433 (1983).
- <sup>15</sup>T. Fujiwara, T. Kugo, H. Terao, S. Uehara, and K. Yamawaki, *Prog. Theor. Phys.* **73**, 926 (1985).
- <sup>16</sup>S. Furui, R. Kobayashi, and K. Ujiiie, *Prog. Theor. Phys.* **76**, 963 (1986).
- <sup>17</sup>S. H. Lee and I. Zahed, *Phys. Rev. D* **37**, 1963 (1988).
- <sup>18</sup>T. H. R. Skyrme, *Nucl. Phys.* **31**, 556 (1962).
- <sup>19</sup>M. Gari and W. Krümpelmann, *Z. Phys. A* **322**, 689 (1985); *Phys. Lett. B* **173**, 10 (1986).
- <sup>20</sup>L. A. Ahrends *et al.*, *Phys. Lett. B* **202**, 284 (1988).
- <sup>21</sup>J.-P. Blaizot, M. Rho, and N. N. Scoccola, *Phys. Lett. B* **209**, 27 (1988).
- <sup>22</sup>N. Kaiser, U. Vogl, W. Weise, and Ulf-G. Meissner, *Nucl. Phys.* **A484**, 593 (1988).
- <sup>23</sup>See, e.g., W. Ruckstuhl *et al.*, *Phys. Rev. Lett.* **56**, 2133 (1986).
- <sup>24</sup>R. Machleidt, K. Holinde, and C. Elster, *Phys. Rep.* **149**, 1 (1987).
- <sup>25</sup>J. W. Durso, M. Saarela, G. E. Brown, and A. D. Jackson, *Nucl. Phys.* **A278**, 445 (1977); J. W. Durso, A. D. Jackson, and B. J. Verwest, *Nucl. Phys.* **A282**, 404 (1977); W. Nutt *et al.*, *ibid.* **B104**, 98 (1976).
- <sup>26</sup>W. Grein, *Nucl. Phys.* **B131**, 255 (1977).
- <sup>27</sup>Ulf-G. Meissner, N. Kaiser, A. Wirzba, and W. Weise, *Phys. Rev. Lett.* **57**, 1676 (1986).
- <sup>28</sup>G. E. Brown and A. D. Jackson, *The Nucleon-Nucleon Interaction* (North-Holland, Amsterdam, 1976).
- <sup>29</sup>See, e.g., J. Ashman *et al.*, *Phys. Lett. B* **206**, 364 (1988); F. E. Close and R. G. Roberts, *Phys. Rev. Lett.* **60**, 1471 (1988); S. J. Brodsky, J. Ellis, and M. Karliner, *Phys. Lett. B* **206**, 309 (1988); H. Høgaasen and F. Myhrer, *ibid.*, **214**, 123 (1988); Z. Ryzak, Northeastern University Report No. NUB-2955, 1988 (unpublished).
- <sup>30</sup>See, e.g., J. F. Donoghue and C. R. Nappi, *Phys. Lett.* **168B**, 105 (1986); R. L. Jaffe and C. L. Korpa, *Commun. Nucl. Part. Phys.* **17**, 163 (1987); V. Bernard, R. L. Jaffe, and Ulf-G. Meissner, *Nucl. Phys.* **B308**, 713 (1988).
- <sup>31</sup>R. Koch, *Z. Phys. C* **15**, 161 (1982).
- <sup>32</sup>C. A. Dominguez and B. J. Verwest, *Phys. Lett.* **89B**, 333 (1980); C. A. Dominguez, *Phys. Rev. C* **24**, 2611 (1981).
- <sup>33</sup>J. Bernabéu, *Nucl. Phys.* **A373**, 593c (1982).
- <sup>34</sup>U. Vogl, diploma thesis, University of Regensburg, 1988.
- <sup>35</sup>E. G. Adelberger and W. C. Haxton, *Annu. Rev. Nucl. Part. Sci.* **35**, 501 (1988).
- <sup>36</sup>M. Bini *et al.*, *Phys. Rev. Lett.* **35**, 797 (1985); E. Evans *et al.*, *ibid.* **35**, 791 (1985).
- <sup>37</sup>W. C. Haxton, in *Proceedings of the Workshop on Parity Violation in Hadronic Systems*, Vancouver, 1987, edited by S. A. Page, W. D. Ramsay, and W. T. H. van Oers (TRIUMF, Vancouver, 1987).
- <sup>38</sup>B. Desplanques, J. F. Donoghue, and B. R. Holstein, *Ann. Phys. (N.Y.)* **124**, 449 (1980).
- <sup>39</sup>V. M. Dubovik and S. V. Zenkin, *Ann. Phys. (N.Y.)* **172**, 100 (1986).
- <sup>40</sup>E. G. Adelberger *et al.*, *Phys. Rev. C* **27**, 2833 (1983).
- <sup>41</sup>S. Galster *et al.*, *Nucl. Phys.* **B32**, 221 (1971).
- <sup>42</sup>H. Feshbach and E. Lomon, *Rev. Mod. Phys.* **39**, 611 (1967).